Matching algorithms and superpixels for image analysis and processing

Rémi Giraud

PhD Defense

29 November 2017

Supervision: Nicolas Papadakis et Vinh-Thong Ta

université de BORDEAUX

Institut de Mathématiques de Bordeaux

LaBRI

Many domains, for many applications:

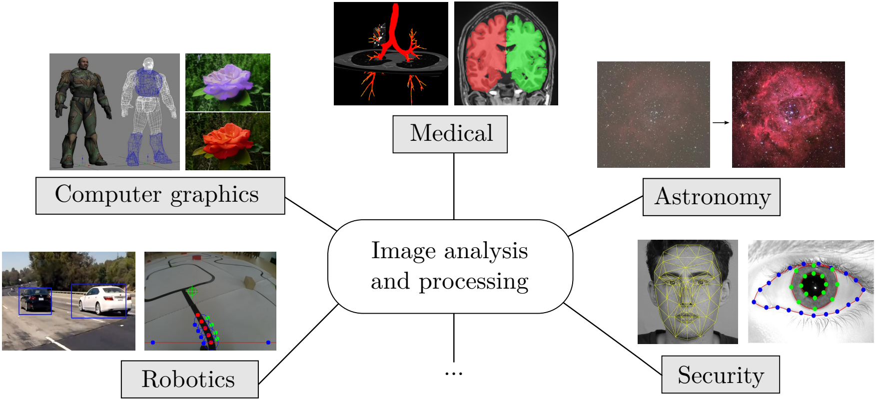

Goal: To automatically generate a result for an input data.

Segmentation and labeling example:

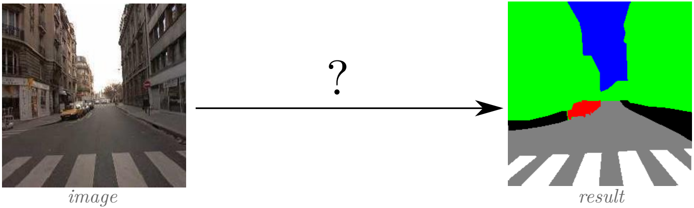

Introduction

Goal: To automatically generate a result for an input data.

Segmentation and labeling example:

→ Necessity to use a extern source of information.

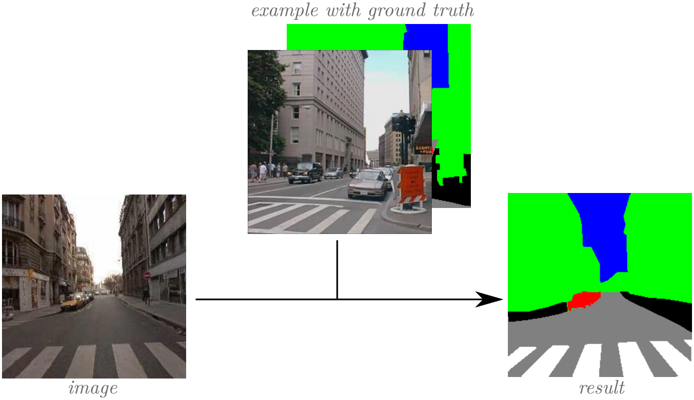

Non-local patch-based methods:

Search for matches for each pixel (patch) of the input image.

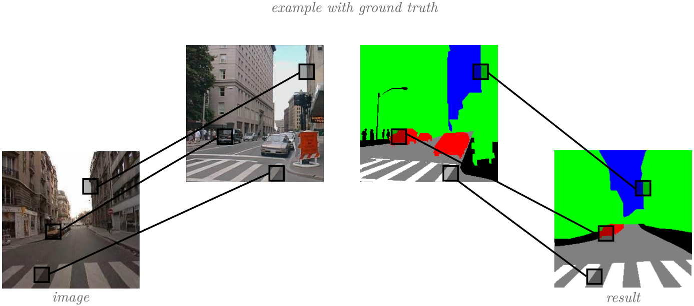

Non-local patch-based methods:

Search for matches for each pixel (patch) of the input image.

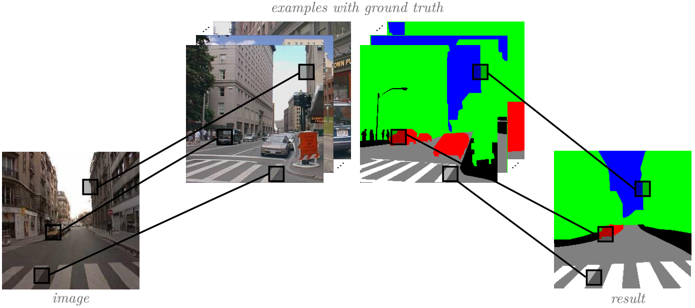

Non-local patch-based methods:

Search for matches for each pixel (patch) of the input image.

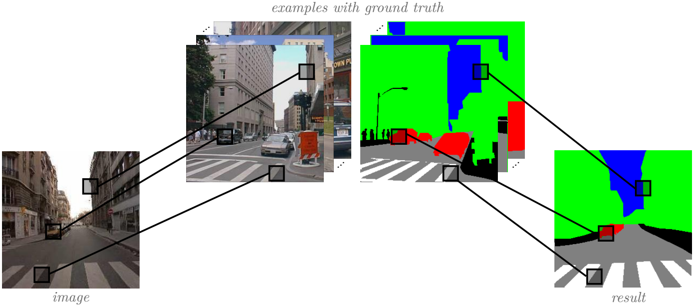

Stake n°1: To propose an algorithm that computes these matches:

- in a library of example images

Non-local patch-based methods:

Search for matches for each pixel (patch) of the input image.

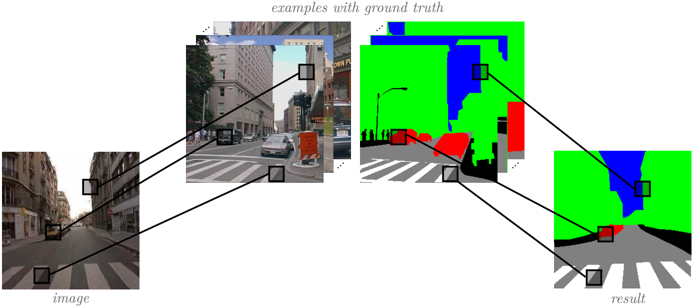

Stake n°1: To propose an algorithm that computes these matches:

- in a library of example images
- without learning step

Non-local patch-based methods:

Search for matches for each pixel (patch) of the input image.

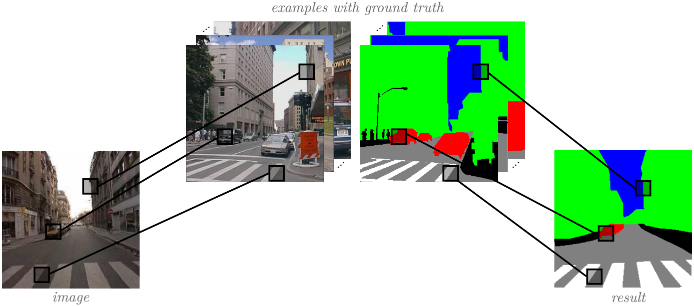

Stake n°1: To propose an algorithm that computes these matches:

- in a library of example images
- without learning step
- in a fast way

Introduction

Data sometimes sizeable and high computational times.

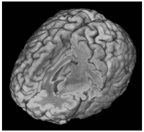

3D volume

HD image

Video

Data sometimes sizeable and high computational times.

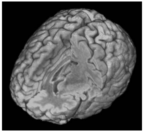

3D volume

HD image

Video

→ Methods to reduce the resolution

- Regular multi-resolution :
  Decompose the image into regular blocks.

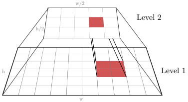

Image

Decomposition into blocks

Average colors

Introduction

Data sometimes sizeable and high computational times.

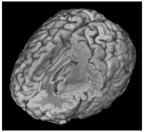

3D volume

HD image

Video

→ Methods to reduce the resolution

- Superpixels (since [Ren and Malik, 2003]):
  Local grouping of pixels with homogeneous colors.

Image

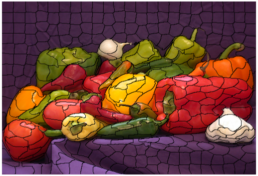

Decomposition into superpixels

Average colors

Data sometimes sizeable and high computational times.

3D volume HD image Video

→ Methods to reduce the resolution

- Superpixels (since [Ren and Malik, 2003]):
  Local grouping of pixels with homogeneous colors.

Image Decomposition into superpixels Average colors

Stake n°2: Irregularity of the decomposition.
→ Limits their use into methods using neighborhood.

- Cerebral images for neurodegenerative diseases (*e.g.*, Alzheimer).
- Analysis of impacted structures necessary for patient follow-up.
  - Manual segmentation very time consuming.
  - High inter-expert variability.

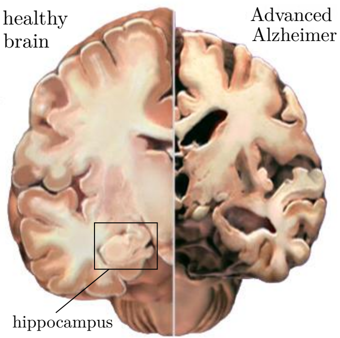

$\rightarrow$ To propose automatic, precise and fast segmentation methods.

Context

- Cerebral images for neurodegenerative diseases (*e.g.*, Alzheimer).
- Analysis of impacted structures necessary for patient follow-up.
  - Manual segmentation very time consuming.
  - High inter-expert variability.

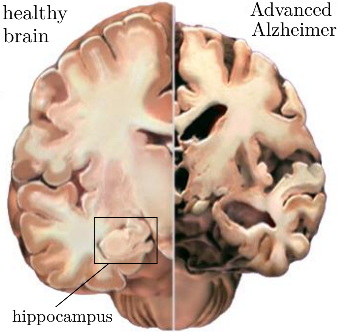

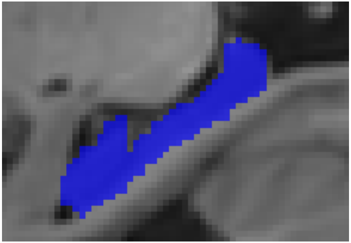

→ To propose automatic, precise and fast segmentation methods.

Computation of non-linear transformation.
Deformation of the model's structure.
[Collins et al., 1995]

→ Very important computational time (hours).

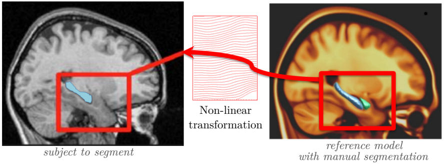

Computation of non-linear transformation.
Deformation of the model's structure.
[Collins et al., 1995]

→ Very important computational time (hours).

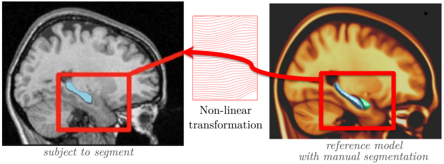

Multi-template approach. [Heckemann et al., 2006]

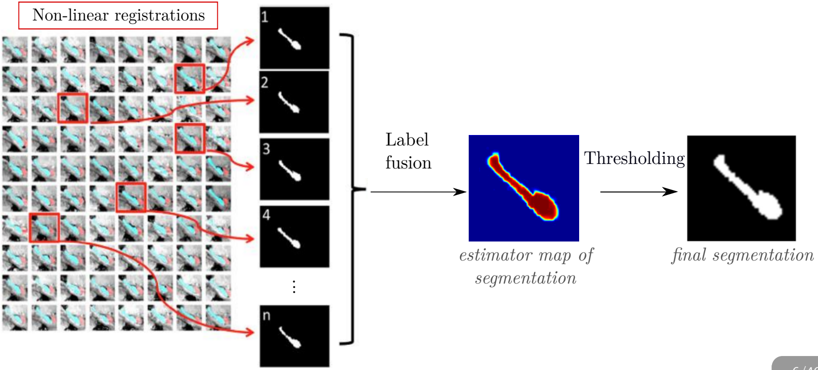

Linear registration (minutes).

Weighted average of the model's patches in a restricted search area.

Label fusion ([Buades et al., 2005]):

$$\mathcal{L}(\mathbf{x_i}) = \frac{\sum_{\{\mathbf{x_j}\}} \omega(P(\mathbf{x_i}),P(\mathbf{x_j}))L(\mathbf{x_j})}{\sum_{\{\mathbf{x_j}\}} \omega(P(\mathbf{x_i}),P(\mathbf{x_j}))}$$

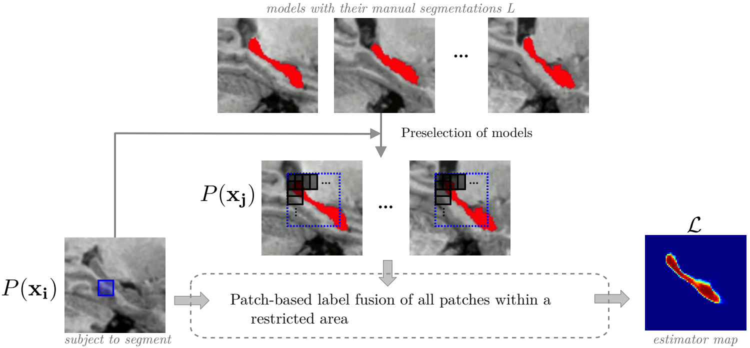

→ Necessary preselection and high number of considered dissimilar patches.

→ Computational time ≈ 10mn by subject.

Linear registration (minutes).

Weighted average of the model's patches in a restricted search area.

Label fusion ([Buades et al., 2005]):

$$\mathcal{L}(\mathbf{x_i}) = \frac{\sum_{\{\mathbf{x_j}\}} \omega(P(\mathbf{x_i}), P(\mathbf{x_j})) L(\mathbf{x_j})}{\sum_{\{\mathbf{x_j}\}} \omega(P(\mathbf{x_i}), P(\mathbf{x_j}))}$$

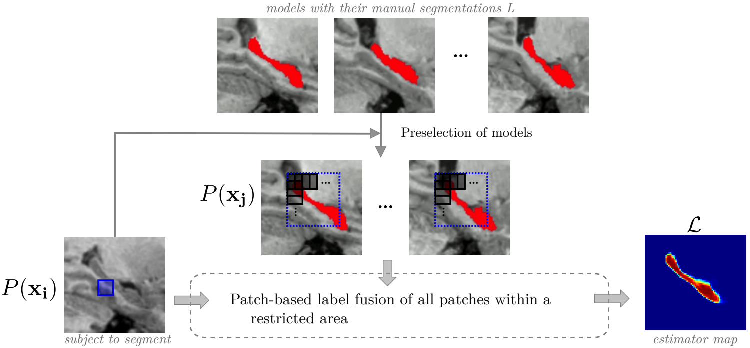

Proposition: To use a fast matching algorithm to compute several good matches within the models.

Choice of the PatchMatch algorithm [Barnes et al., 2009]:

Computation of a match in B for each patch of A.

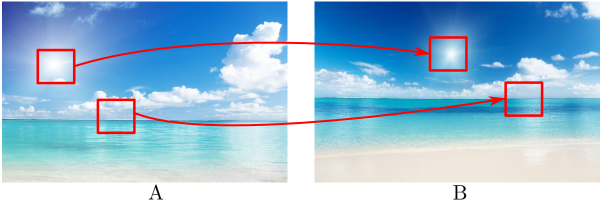

State-of-the-art - Matching algorithm

Choice of the PatchMatch algorithm [Barnes et al., 2009]:

Computation of a match in B for each patch of A.

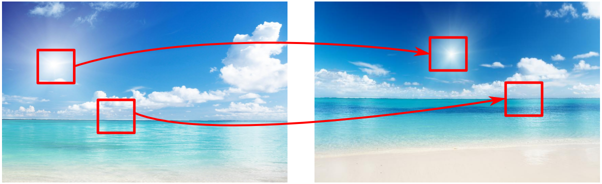

A B

Key idea: To use the information from adjacent patches to propagate good matches.

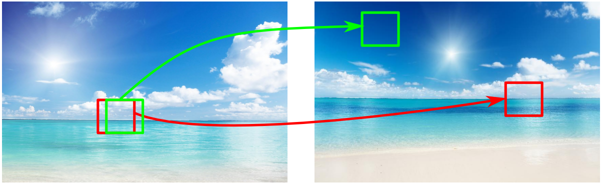

A B

$\rightarrow$ The complexity of the algorithm only depends on the size of the image A.

State-of-the-art - Matching algorithm

Choice of the PatchMatch algorithm [Barnes et al., 2009]:

Computation of a match in B for each patch of A.

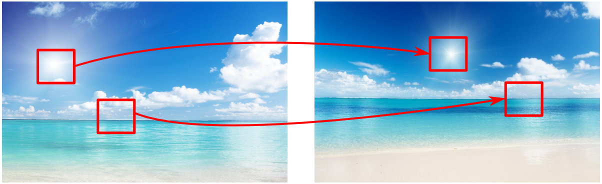

A B

Key idea: To use the information from adjacent patches to propagate good matches.

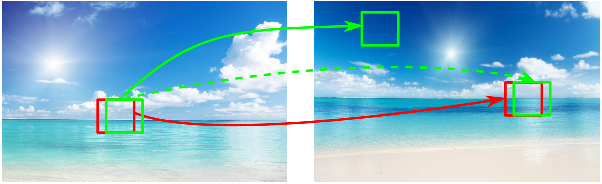

A B

$\rightarrow$ The complexity of the algorithm only depends on the size of the image A.

Linear registration (minutes).

Weighted average of models patches in a restricted search area.

Label fusion ([Buades et al., 2005]):

$$\mathcal{L}(\mathbf{x_i}) = \frac{\sum_{\{\mathbf{x_j}\}} \omega(P(\mathbf{x_i}), P(\mathbf{x_j}))L(\mathbf{x_j})}{\sum_{\{\mathbf{x_j}\}} \omega(P(\mathbf{x_i}), P(\mathbf{x_j}))}$$

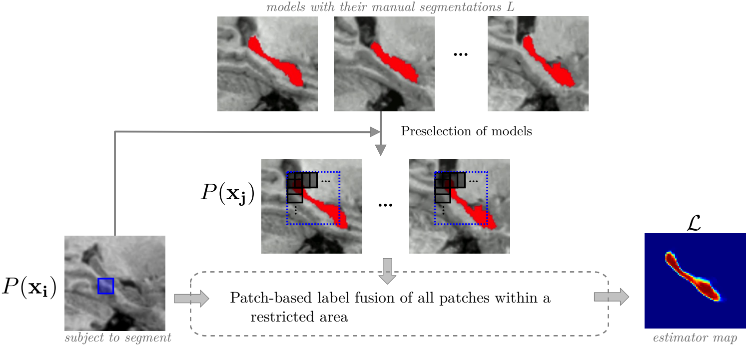

Proposition: To use a fast matching algorithm to compute several good matches within the models.

Linear registration (minutes).

Weighted average of models patches in a restricted search area.

Label fusion ([Buades et al., 2005]):

$$\mathcal{L}(\mathbf{x_i}) = \frac{\sum_{\{\mathbf{x_j}\}} \omega(P(\mathbf{x_i}),P(\mathbf{x_j}))L(\mathbf{x_j})}{\sum_{\{\mathbf{x_j}\}} \omega(P(\mathbf{x_i}),P(\mathbf{x_j}))}$$

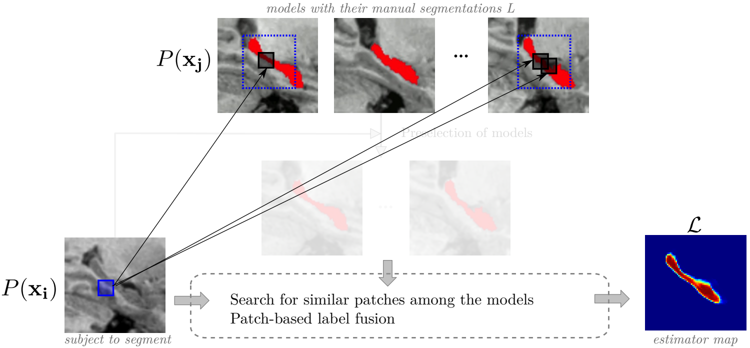

Proposition: To use a fast matching algorithm to compute several good matches within the models.

Optimized PAtchmatch for Label fusion (OPAL)

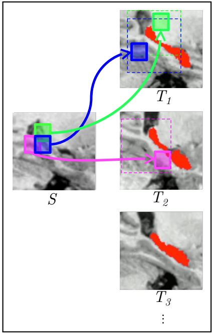

Initialization

Optimized PAtchmatch for Label fusion (OPAL)

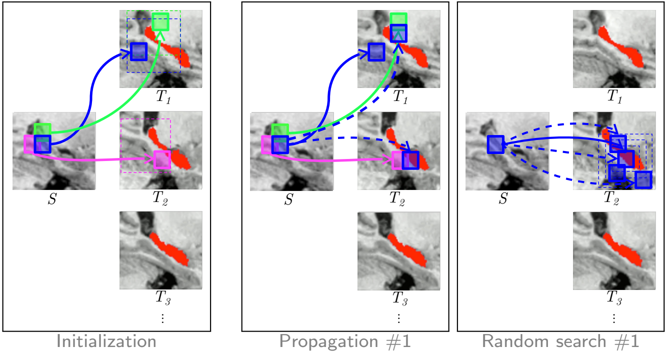

Optimized PAtchmatch for Label fusion (OPAL)

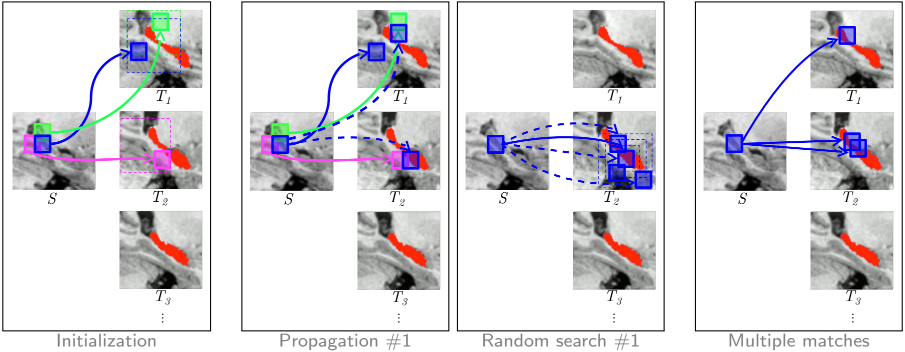

Optimized PAtchmatch for Label fusion (OPAL)

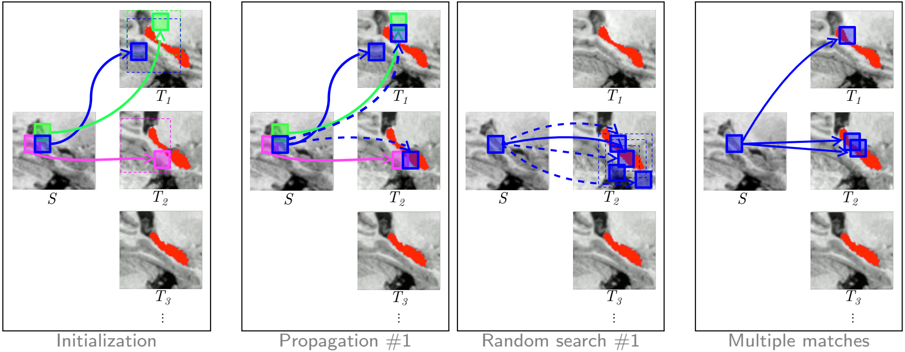

→ Reduced number of patches contributing to the segmentation.
→ No necessary preselection.
→ Reduced computational time.

Independent multi-feature and multi-scale search and fusion.

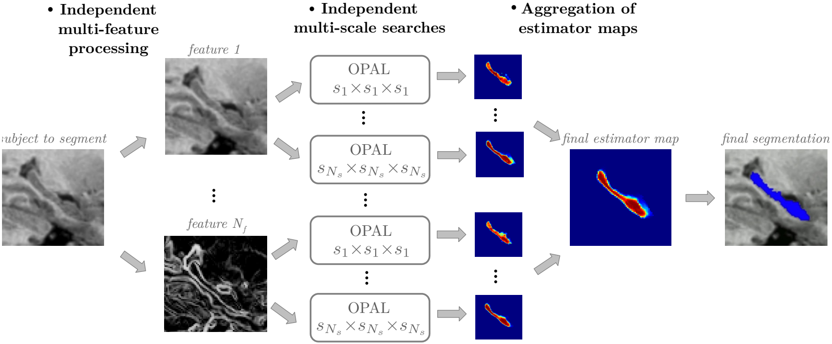

$\rightarrow$ Increase of the segmentation process accuracy.

Segmentation results

Validation metric [Zijdenbos et al., 1994]:

$$\mathrm{Dice}(\mathcal{S}_{\mathrm{expert}}, \mathcal{S}_{\mathrm{auto}}) = \frac{2|\mathcal{S}_{\mathrm{expert}} \cap \mathcal{S}_{\mathrm{auto}}|}{|\mathcal{S}_{\mathrm{expert}}| + |\mathcal{S}_{\mathrm{auto}}|}$$

Validation metric [Zijdenbos et al., 1994]:

$$\text{Dice}(\mathcal{S}_{\text{expert}}, \mathcal{S}_{\text{auto}}) = \frac{2|\mathcal{S}_{\text{expert}} \cap \mathcal{S}_{\text{auto}}|}{|\mathcal{S}_{\text{expert}}| + |\mathcal{S}_{\text{auto}}|}$$

- ICBM dataset: 80 young healthy subjects [Mazziotta et al., 1995]
  Inter-expert variability: 90%.

Method	Median Dice	Computational time
Patch-based [Coupé et al., 2011]	88.2%	$(\times 700)$
Multi-templates [Collins and Pruessner, 2010]	88.6%	$(\times 4300)$
Dictionary learning [Tong et al., 2013]	89.0%	$(\times 1000)$
OPAL (2015)	$\mathbf{90.0\%}$	$\mathbf{0.92s}$

- EADC-ADNI: 100 healthy and unhealthy subjects [Boccardi et al., 2014]
  Inter-expert variability: 89%.

Method	Average Dice	Computational time
Random Forest [Tangaro et al., 2014]	76.0%	$\times$
Multi-templates [Gray et al., 2014]	87.6%	$\times$
Patch-based [Zhu et al., 2017]	88.3%	$\times$
Multi-scale patch-based [Pant et al., 2015]	89.2%	$(\times 200)$
OPAL (2015)	$\mathbf{89.8\%}$	$\mathbf{1.48s}$

Median subject
Dice $= 89.9\%$

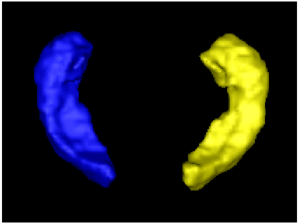

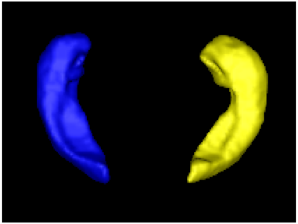

Initial image

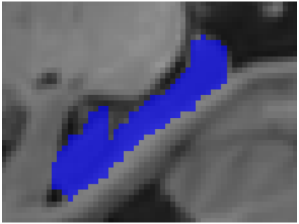

$\mathcal{S}_{\text{expert}}$

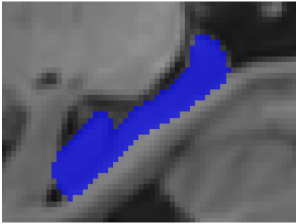

$\mathcal{S}_{\text{opal}}$

- PatchMatch for a library of 3D images
- New automatic segmentation method
- Results > inter-expert variability in a few seconds

Associated publications:

- Vinh-Thong Ta, Rémi Giraud, D. Louis Collins, and Pierrick Coupé.
  Optimized PatchMatch for near real time and accurate label fusion.
  Proc. of Int. Conf. on Medical Image Computing and Computer-Assisted Intervention (MICCAI), pages 105–112, 2014.
- Rémi Giraud, Vinh-Thong Ta, Nicolas Papadakis, D. Louis Collins, and Pierrick Coupé.
  Optimisation de l'algorithme PatchMatch pour la segmentation de structures anatomiques.
  Actes du Groupe d'Études du Traitement du Signal et des Images (GRETSI), 2015.
- Rémi Giraud, Vinh-Thong Ta, Nicolas Papadakis, Jose V. Manjón, D. Louis Collins, and Pierrick Coupé.
  An optimized PatchMatch for multi-scale and multi-feature label fusion.
  NeuroImage (NIMG), 124:770–782, 2016.

- Extension to the cerebellum segmentation [Manjón et al., 2017] [Romero et al., 2017]
- Extension to the Alzheimer's disease prediction [Hett et al., 2016]
- Integration into the online platform volBrain [Manjón et Coupé, 2016]

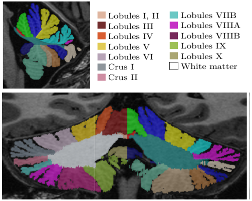

Associated publications:

- Kilian Hett, Vinh-Thong Ta, Rémi Giraud, Mary Mondino, Jose V. Manjón, and Pierrick Coupé.
  Patch-based DTI grading: Application to alzheimer's disease classification.
  Proc. of Int. Work. on Patch-based Techniques in Medical Imaging (Patch-MI, MICCAI), pages 76–83, 2016.
- Jose V. Manjón, Pierrick Coupé, Jose E. Romero, Vinh-Thong Ta, and Rémi Giraud.
  Ceres: A new cerebellum lobule segmentation method.
  Dépot logiciel : IDDN.FR.001.470008.000.S.P.2015.000.21000, 2016.
- Jose E. Romero, Pierrick Coupé, Rémi Giraud, Vinh-Thong Ta, Vladimir Fonov, and Min Tae M. Park, et al.
  CERES: A new cerebellum lobule segmentation method.
  NeuroImage (NIMG), 147:916–924, 2017.

Extensions of OPAL

- Extension to the cerebellum segmentation [Manjón et al., 2017] [Romero et al., 2017]
- Extension to the Alzheimer's disease prediction [Hett et al., 2016]
- Integration into the online platform volBrain [Manjón et Coupé, 2016]

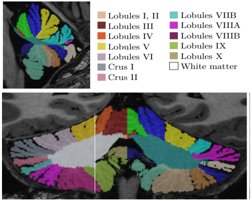

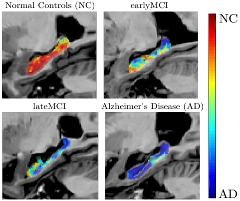

Associated publications:

- Kilian Hett, Vinh-Thong Ta, Rémi Giraud, Mary Mondino, Jose V. Manjón, and Pierrick Coupé.
  Patch-based DTI grading: Application to alzheimer's disease classification.
  Proc. of Int. Work. on Patch-based Techniques in Medical Imaging (Patch-MI, MICCAI), pages 76–83, 2016.
- Jose V. Manjón, Pierrick Coupé, Jose E. Romero, Vinh-Thong Ta, and Rémi Giraud.
  Ceres: A new cerebellum lobule segmentation method.
  Dépot logiciel : IDDN.FR.001.470008.000.S.P.2015.000.21000, 2016.
- Jose E. Romero, Pierrick Coupé, Rémi Giraud, Vinh-Thong Ta, Vladimir Fonov, and Min Tae M. Park, et al.
  CERES: A new cerebellum lobule segmentation method.
  NeuroImage (NIMG), 147:916–924, 2017.

- Extension to the cerebellum segmentation [Manjón et al., 2017] [Romero et al., 2017]
- Extension to the Alzheimer's disease prediction [Hett et al., 2016]
- Integration into the online platform volBrain [Manjón et Coupé, 2016]

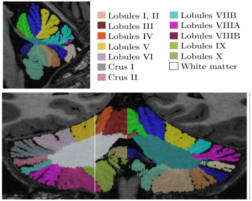

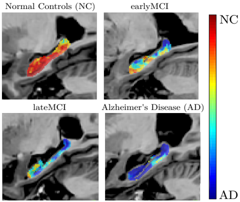

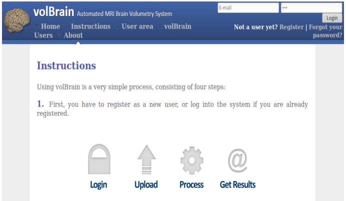

Associated publications:

- Kilian Hett, Vinh-Thong Ta, Rémi Giraud, Mary Mondino, Jose V. Manjón, and Pierrick Coupé.
  Patch-based DTI grading: Application to alzheimer's disease classification.
  Proc. of Int. Work. on Patch-based Techniques in Medical Imaging (Patch-MI, MICCAI), pages 76–83, 2016.
- Jose V. Manjón, Pierrick Coupé, Jose E. Romero, Vinh-Thong Ta, and Rémi Giraud.
  Ceres: A new cerebellum lobule segmentation method.
  Dépot logiciel : IDDN.FR.001.470008.000.S.P.2015.000.21000, 2016.
- Jose E. Romero, Pierrick Coupé, Rémi Giraud, Vinh-Thong Ta, Vladimir Fonov, and Min Tae M. Park, et al.
  CERES: A new cerebellum lobule segmentation method.
  NeuroImage (NIMG), 147:916–924, 2017.

Adaptation of the PatchMatch algorithm to superpixels:

- Similar initialization and random search.
- Propagation: necessity to preserve the relative positions between adjacent neighbors.

 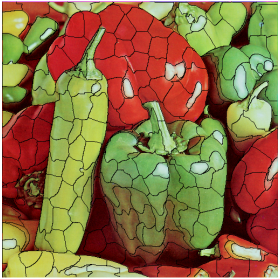

Adaptation of the PatchMatch algorithm to superpixels:

- Similar initialization and random search.
- Propagation: necessity to preserve the relative positions between adjacent neighbors.

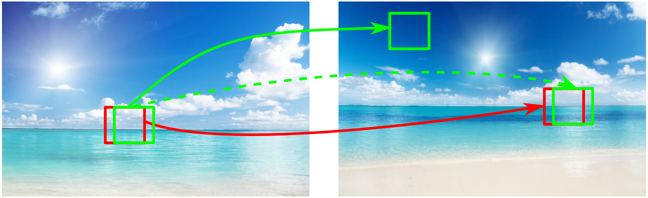

A B

Adaptation of the PatchMatch algorithm to superpixels:

- Similar initialization and random search.
- Propagation: necessity to preserve the relative positions between adjacent neighbors.

  $\rightarrow$ Selection of the neighbor with the most similar orientation.

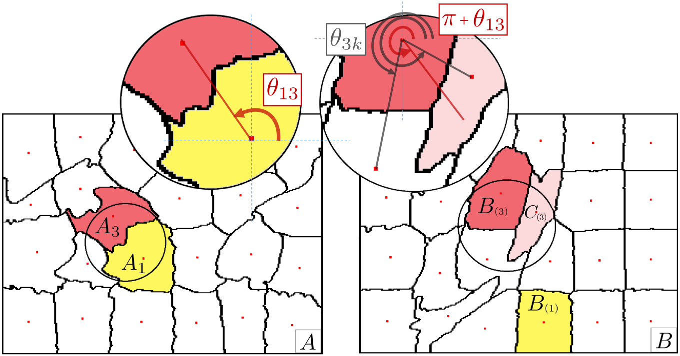

$\rightarrow$ SuperPatchMatch: fast search algorithm of superpixel-based matches.

Constraints:

- Reduced computational time (HD, video)
- Global transfer of the source color palette
- Respect of the target structures


Source image


Target image


Transfer result

Application to color transfer

Constraints:

- Reduced computational time (HD, video)
- Global transfer of the source color palette
- Respect of the target structures

Superpixel-based Color Transfer (SCT):

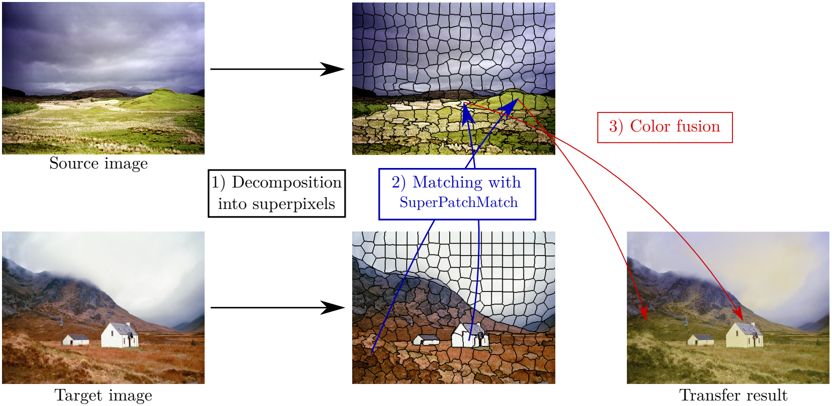

Constraints:

- Reduced computational time (HD, video)
- Global transfer of the source color palette
- Respect of the target structures

Superpixel-based Color Transfer (SCT):

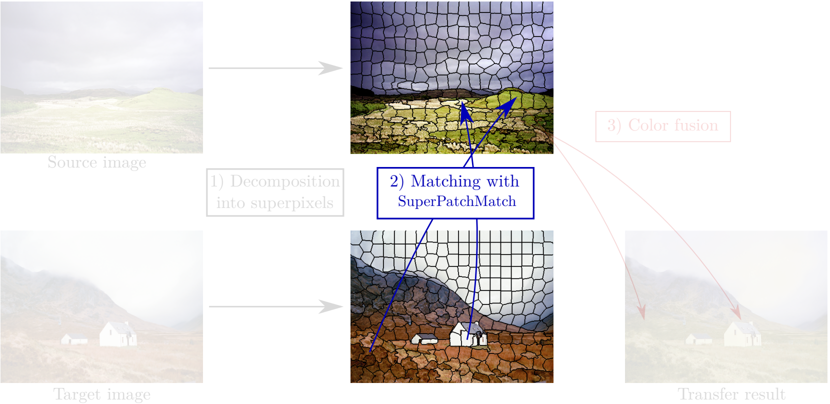

Problem:

No control of the distribution of selected superpixels in the source image.

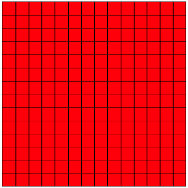

Target image

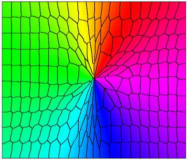

Source image

Without constraint

Transfer result
(average colors)

Selected superpixels

Application to color transfer

Problem:

No control of the distribution of selected superpixels in the source image.

Solution:

To constrain a source superpixel to be selected no more than ϵ times.

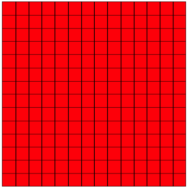

Target image

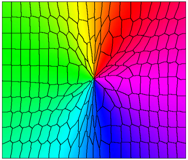

Source image

Without constraint ($\epsilon = \infty$)

Transfer result (average colors)

Selected superpixels

With constraint ($\epsilon = 1$)

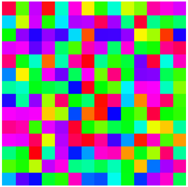

Transfer result (average colors)

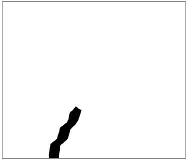

Selected superpixels

Application to color transfer - Results

Comparison to:

- Optimal transport [Pitié et al., 2007]
- Relaxed optimal transport [Rabin et al., 2014]
- 3D color gamut mapping [Nguyen et al., 2014]

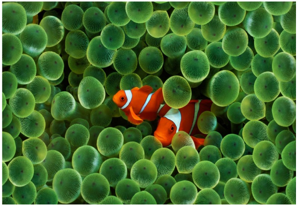

Target image

Source image

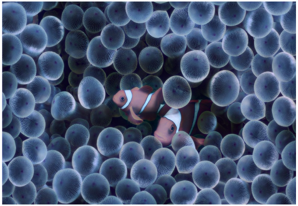

SCT

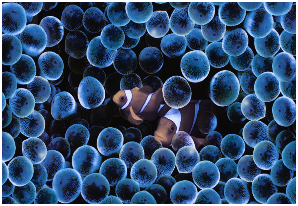

[Pitié et al., 2007]

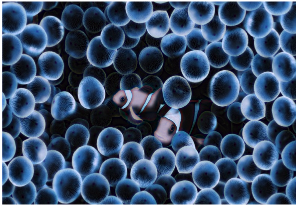

[Rabin et al., 2014]

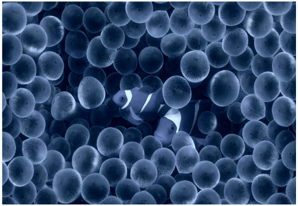

[Nguyen et al., 2014]

Application to color transfer - Results

Comparison to:

- Optimal transport [Pitié et al., 2007]
- Relaxed optimal transport [Rabin et al., 2014]
- 3D color gamut mapping [Nguyen et al., 2014]

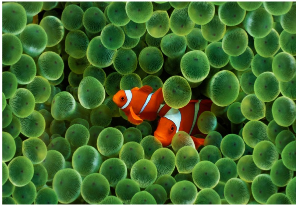

Target image

Source image

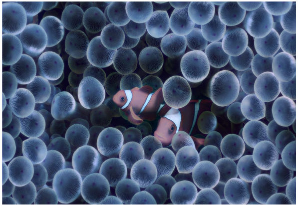

SCT

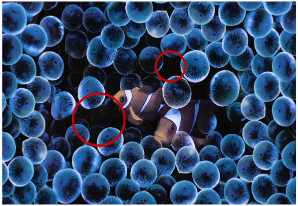

[Pitié et al., 2007]

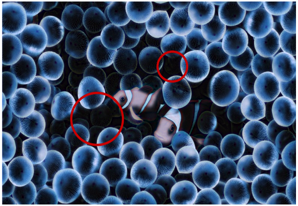

[Rabin et al., 2014]

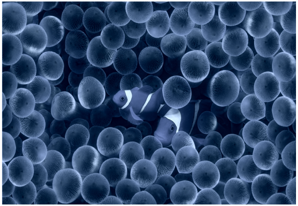

[Nguyen et al., 2014]

Application to color transfer - Results

Comparison to:

- Optimal transport [Pitié et al., 2007]
- Relaxed optimal transport [Rabin et al., 2014]
- 3D color gamut mapping [Nguyen et al., 2014]

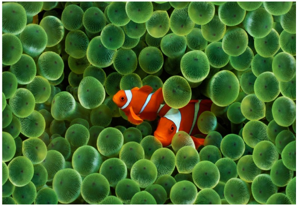

Target image

Source image

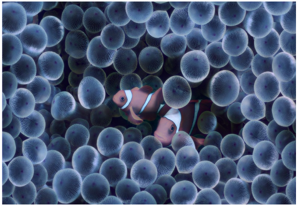

SCT

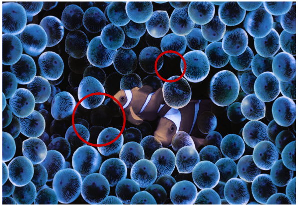

[Pitié et al., 2007]

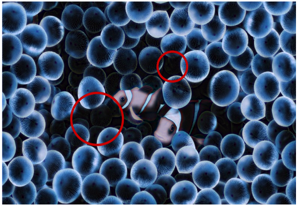

[Rabin et al., 2014]

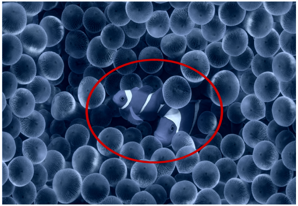

[Nguyen et al., 2014]

Application to color transfer - Results

Comparison to:

- Optimal transport [Pitié et al., 2007]
- Relaxed optimal transport [Rabin et al., 2014]
- 3D color gamut mapping [Nguyen et al., 2014]

Target image

Source image

SCT

[Pitié et al., 2007]

[Rabin et al., 2014]

[Nguyen et al., 2014]

Application to color transfer - Results

Comparison to:

- Optimal transport [Pitié et al., 2007]
- Relaxed optimal transport [Rabin et al., 2014]
- 3D color gamut mapping [Nguyen et al., 2014]

Target image

Source image

SCT

[Pitié et al., 2007]

[Rabin et al., 2014]

[Nguyen et al., 2014]

Application to color transfer - Results

Comparison to:

- Optimal transport [Pitié et al., 2007]
- Relaxed optimal transport [Rabin et al., 2014]
- 3D color gamut mapping [Nguyen et al., 2014]

Target image

Source image

SCT

[Pitié et al., 2007]

[Rabin et al., 2014]

[Nguyen et al., 2014]

Comparison to:

- Optimal transport [Pitié et al., 2007]
- Relaxed optimal transport [Rabin et al., 2014]
- 3D color gamut mapping [Nguyen et al., 2014]

Target image

Source image

SCT

[Pitié et al., 2007]

[Rabin et al., 2014]

[Nguyen et al., 2014]

Superpixel-based matches:

→ No use of the neighborhood, loss of spatial consistency.

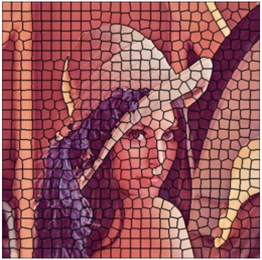

Decomposition 1

Decomposition 2

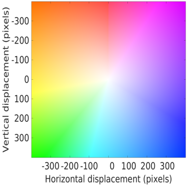

Optical flow representation

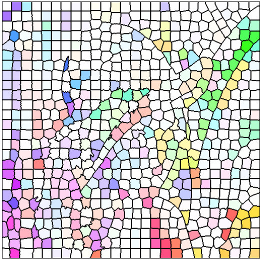

Superpixel-based

Superpixel-based matches:

→ No use of the neighborhood, loss of spatial consistency.

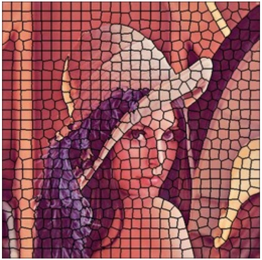

Decomposition 1

Decomposition 2

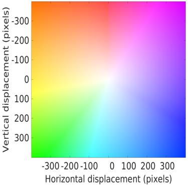

Optical flow representation

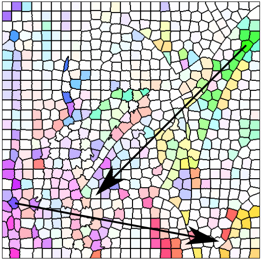

Superpixel-based

Usual distance between regular patches:

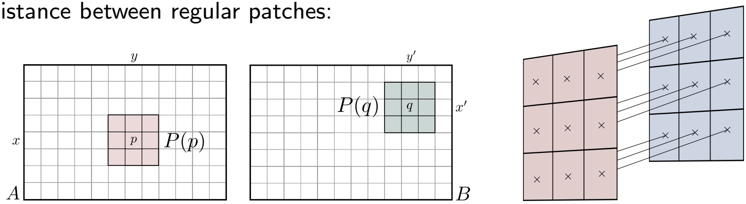

Sum of squared differences (patches of size $(2s+1)^2$):

$$D(P(p),P(q)) = \sum_{i=-s}^{s}\sum_{j=-s}^{s}\big(A(x+i,y+j) - B(x'+i,y'+j)\big)^2$$

Impact of the neighborhood

Usual distance between regular patches:

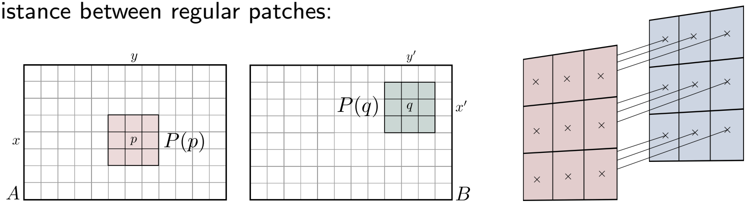

Sum of squared differences (patches of size $(2s+1)^2$):

$$D(P(p),P(q)) = \sum_{i=-s}^{s}\sum_{j=-s}^{s}\left(A(x+i,y+j) - B(x'+i,y'+j)\right)^2$$

How to adapt to superpixels?

- Neighborhood structure preserving the geometry
- Comparison between two elements

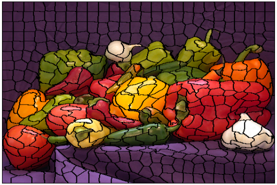

- Definition:

All superpixels $A_{i'}$ with their barycenter $c_{i'}$ contained into a R radius.

$\mathbf{A_i}$ superpatch of superpixel A_i:

$$\mathbf{A_i} = \{A_{i'}, \text{ such that } ||c_i - c_{i'}||_2 \leq R\}$$

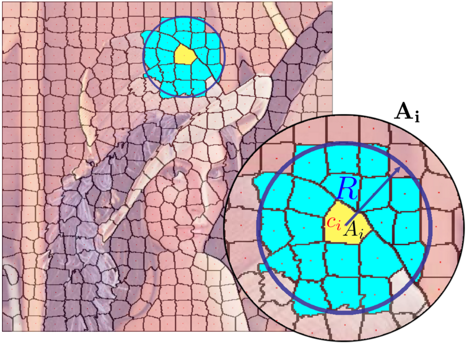

- Comparison of two superpatches $\mathbf{A_i}$ et $\mathbf{B_j}$:

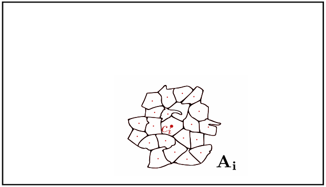

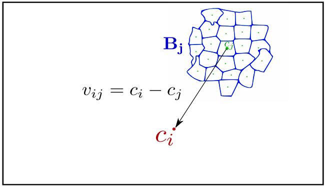

Dissimilarity measure:

$$D(\mathbf{A_i},\mathbf{B_j}) = \frac{\sum\limits_{A_{i'}\in\mathbf{A_i}}\sum\limits_{B_{j'}\in\mathbf{B_j}} w(A_{i'},B_{j'})d(F^A_{i'},F^B_{j'})}{\sum\limits_{A_{i'}\in\mathbf{A_i}}\sum\limits_{B_{j'}\in\mathbf{B_j}} w(A_{i'},B_{j'})}$$

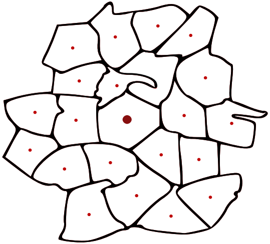

Spatial weighting between registered barycenters:

$$w(A_{i'},B_{j'}) = \exp^{-\frac{\|c_{i'}-c_{j'}-v_{ij}\|_2^2}{\sigma^2}}$$

- Comparison of two superpatches $\mathbf{A_i}$ et $\mathbf{B_j}$:

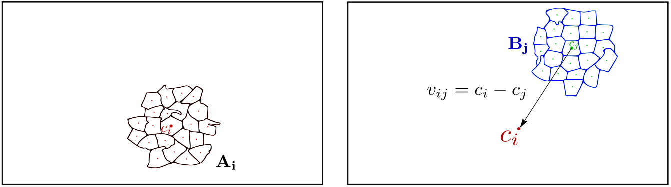

Dissimilarity measure:

$$D(\mathbf{A_i},\mathbf{B_j}) = \frac{\sum_{A_{i'} \in \mathbf{A_i}} \sum_{B_{j'} \in \mathbf{B_j}} w(A_{i'}, B_{j'}) d(F^A_{i'}, F^B_{j'})}{\sum_{A_{i'} \in \mathbf{A_i}} \sum_{B_{j'} \in \mathbf{B_j}} w(A_{i'}, B_{j'})}$$

Spatial weighting between registered barycenters:

$$w(A_{i'}, B_{j'}) = \exp^{-\frac{\|c_{i'} - c_{j'} - v_{ij}\|_2^2}{\sigma^2}}$$

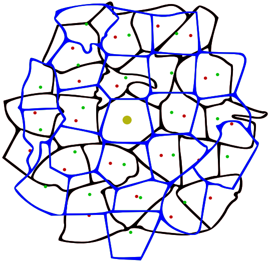

- Comparison of two superpatches $\mathbf{A_i}$ et $\mathbf{B_j}$:

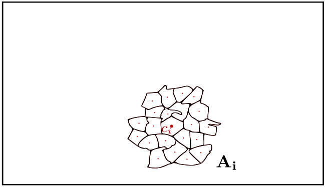

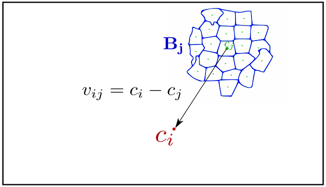

Dissimilarity measure:

$$D(\mathbf{A_i},\mathbf{B_j}) = \frac{\sum\limits_{A_{i'}\in\mathbf{A_i}} \sum\limits_{B_{j'}\in\mathbf{B_j}} w(A_{i'},B_{j'})\, d(F^A_{i'},F^B_{j'})}{\sum\limits_{A_{i'}\in\mathbf{A_i}} \sum\limits_{B_{j'}\in\mathbf{B_j}} w(A_{i'},B_{j'})}$$

Spatial weighting between registered barycenters:

$$w(A_{i'},B_{j'}) = \exp^{-\frac{\|c_{i'}-c_{j'}-v_{ij}\|_2^2}{\sigma^2}}$$

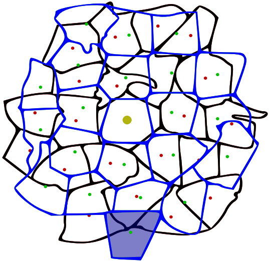

- Comparison of two superpatches $\mathbf{A_i}$ et $\mathbf{B_j}$:

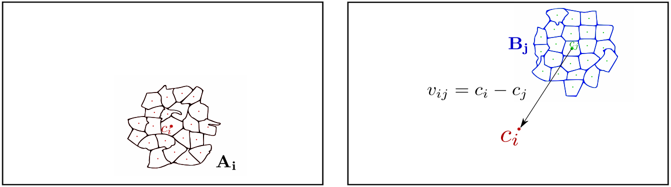

Dissimilarity measure:

$$D(\mathbf{A_i},\mathbf{B_j}) = \frac{\sum\limits_{A_{i'}\in\mathbf{A_i}} \sum\limits_{B_{j'}\in\mathbf{B_j}} w(A_{i'},B_{j'})\, d(F^A_{i'},F^B_{j'})}{\sum\limits_{A_{i'}\in\mathbf{A_i}} \sum\limits_{B_{j'}\in\mathbf{B_j}} w(A_{i'},B_{j'})}$$

Spatial weighting between registered barycenters:

$$w(A_{i'},B_{j'}) = \exp^{-\frac{\|c_{i'}-c_{j'}-v_{ij}\|_2^2}{\sigma^2}}$$

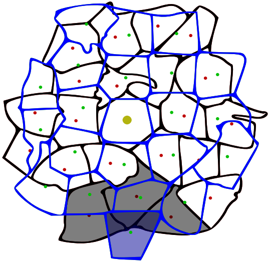

Superpixel-based matches:

→ Spatial consistency with the superpatch.

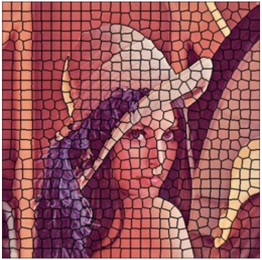

Decomposition 1

Decomposition 2

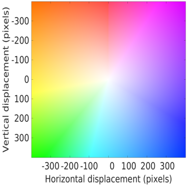

Optical flow representation

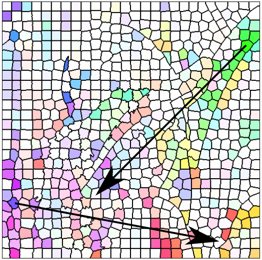

Superpixel-based

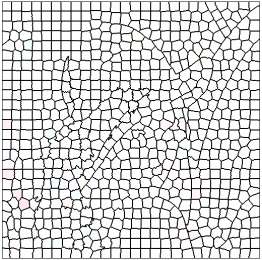

Superpatch-based

LFW dataset [Huang et al., 2007]:

1500 example images and 927 test images.

3 labels: hair, face and background.

Decompositions into superpixels provided.

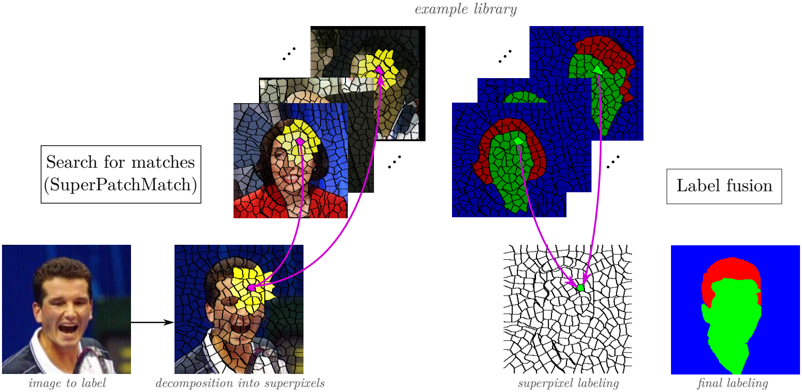

- Impact of the superpatch:

Superpixels | Ground truh | SPM (superpixels) | SPM (superpatches) | Superpixels | Ground truh | SPM (superpixels) | SPM (superpatches)

- Impact of the superpatch:

Superpixels | Ground truh | SPM (superpixels) | SPM (superpatches) | Superpixels | Ground truh | SPM (superpixels) | SPM (superpatches)

- Comparison to state-of-the-art:

Method	Superpixel-wise accuracy	Pixel-wise accuracy
Spatial CRF [Kae et al., 2013]	93.95%	×
CRBM [Kae et al., 2013]	94.10%	×
GLOC [Kae et al., 2013]	94.95%	×
DCNN [Liu et al., 2015]	×	95.24%
SuperPatchMatch (2016)	**95.08%**	**95.43%**

- PatchMatch for superpixels
- Constraint on the distribution of matches

- New superpixel neighborhood structure (superpatch)
- Competitive results with some learning-based methods

Associated publications:

- Rémi Giraud, Vinh-Thong Ta, Aurélie Bugeau, Pierrick Coupé, and Nicolas Papadakis.
  SuperPatchMatch: An algorithm for robust correspondences using superpixel patches.
  IEEE Trans. on Image Processing (TIP), 2017.

- Rémi Giraud, Vinh-Thong Ta, and Nicolas Papadakis.
  Transfert de couleurs basé superpixels.
  Actes du Groupe d'Études du Traitement du Signal et des Images (GRETSI), 2017.

- Rémi Giraud, Vinh-Thong Ta, and Nicolas Papadakis.
  Superpixel-based color transfer.
  Proc. of IEEE International Conference on Image Processing (ICIP), 2017.

- Impact of the superpixel decomposition $\mathcal{S}$:

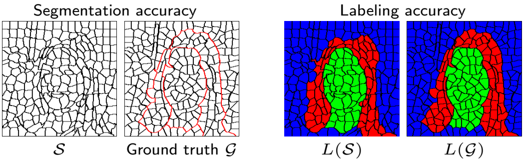

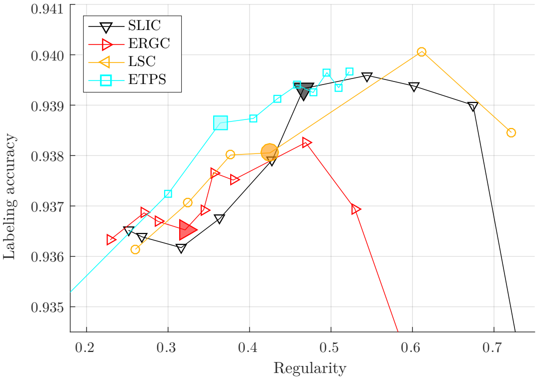

Simple Linear Iterative Clustering (SLIC) [Achanta et al., 2012]

Constrained K-means

Iterative refinement

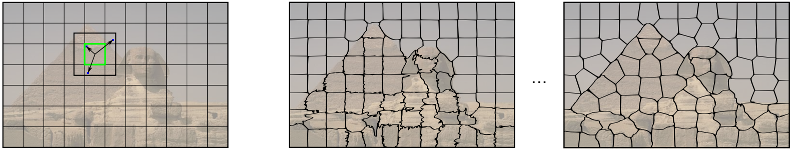

Simple Linear Iterative Clustering (SLIC) [Achanta et al., 2012]

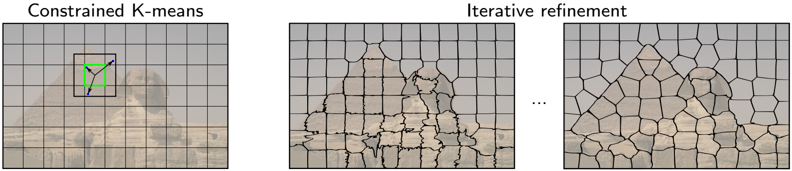

Distance between a pixel p and a superpixel S_k:

$$D(p, S_k) = d_{\text{color}}(F_p, F_{S_k}) + d_{\text{spatial}}(X_p, X_{S_k})m$$

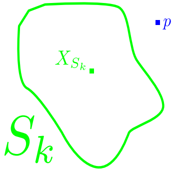

$F_p = [l_p, a_p, b_p]$ color in the CIELab space
$X_p = [x_p, y_p]$ position
F_{S_k}, X_{S_k} average on pixels $\in S_k$
m regularity parameter

Distance between a pixel p and a superpixel S_k:

$$D(p, S_k) = d_{\text{color}}(F_p, F_{S_k}) + d_{\text{spatial}}(X_p, X_{S_k})m$$

Limitations:

- Global regularity parameter $\rightarrow$ irregular shapes with low m.
- No contour information $\rightarrow$ low contour adherence performances.
- Only local pixel color considered $\rightarrow$ no robustness to noise.

$m = 60$

$m = 10$

Distance between a pixel p and a superpixel S_k:

$$D(p, S_k) = d_{\text{color}}(F_p, F_{S_k}) + d_{\text{spatial}}(X_p, X_{S_k})m$$

Limitations:

- Global regularity parameter $\rightarrow$ irregular shapes with low m.
- No contour information $\rightarrow$ low contour adherence performances.
- Only local pixel color considered $\rightarrow$ no robustness to noise.

Distance between a pixel p and a superpixel S_k:

$$D(p, S_k) = d_{\text{color}}(F_p, F_{S_k}) + d_{\text{spatial}}(X_p, X_{S_k})m$$

Limitations:

- Global regularity parameter $\rightarrow$ irregular shapes with low m.
- No contour information $\rightarrow$ low contour adherence performances.
- Only local pixel color considered $\rightarrow$ no robustness to noise.

Initial image

Noisy image

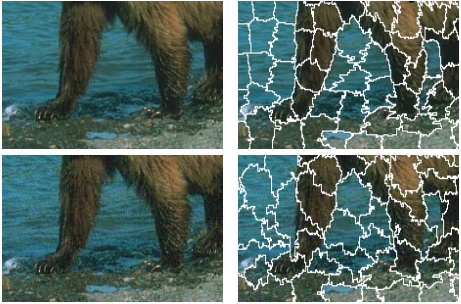

Superpixels with Contour Adherence using Linear Path (SCALP):

- Color and contour distance on the linear path $\mathbf{P}_p^k$ to the barycenter of the superpixel
- Color distance on the pixel neighborhood $V(p)$

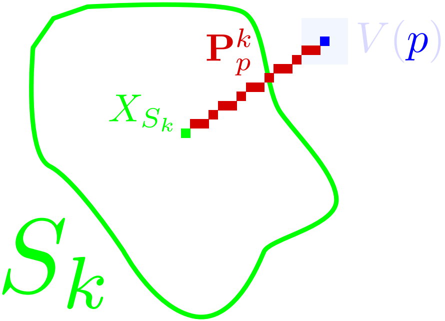

Superpixels with Contour Adherence using Linear Path (SCALP):

- Color and contour distance on the linear path $\mathbf{P}_p^k$ to the barycenter of the superpixel
- Color distance on the pixel neighborhood $V(p)$

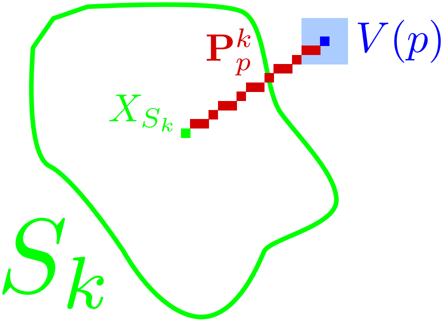

Color distance on linear path $\mathbf{P}_p^k$:

$$d_{\text{path}}(\mathbf{P}_p^k, S_k) = \frac{1}{|\mathbf{P}_p^k|} \sum_{q \in \mathbf{P}_p^k} d_{\text{color}}(F_q, F_{S_k})$$

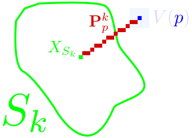

Color distance on linear path $\mathbf{P}_p^k$:

$$d_{\text{path}}(\mathbf{P}_p^k, S_k) = \frac{1}{|\mathbf{P}_p^k|}\sum_{q\in\mathbf{P}_p^k} d_{\text{color}}(F_q, F_{S_k})$$

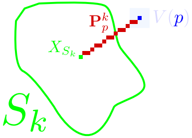

$\rightarrow$ Prevents the appearance of irregular shapes by encouraging convexity.

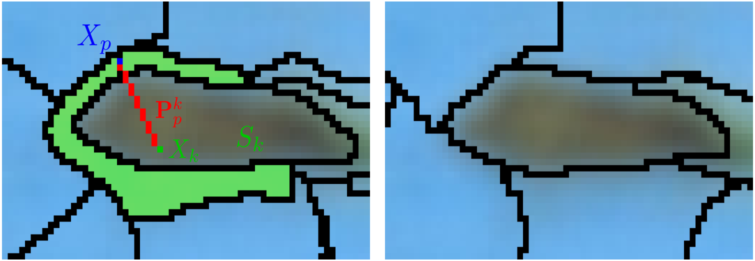

SLIC SCALP

Contour distance on linear path $\mathbf{P}_p^k$:

$$d_{\text{contour}}(\mathbf{P}_p^k) = \gamma \max_{q \in \mathbf{P}_p^k} \mathcal{C}(q)$$

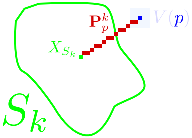

$\rightarrow$ Possible use of a contour map $\mathcal{C}$ to favor the respect of image objects.

Contour distance on linear path $\mathbf{P}_p^k$:

$$d_{\text{contour}}(\mathbf{P}_p^k) = \gamma \max_{q \in \mathbf{P}_p^k} \mathcal{C}(q)$$

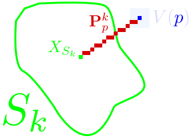

$\rightarrow$ Possible use of a contour map $\mathcal{C}$ to favor the respect of image objects.


Image

Linear path

Max. contour

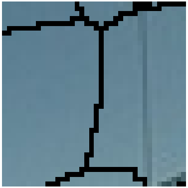
Result

Contour distance on linear path $\mathbf{P}_p^k$:

$$d_{\text{contour}}(\mathbf{P}_p^k) = \gamma \max_{q \in \mathbf{P}_p^k} \mathcal{C}(q)$$

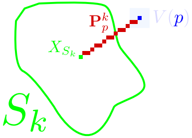

→ Possible use of a contour map $\mathcal{C}$ to favor the respect of image objects.

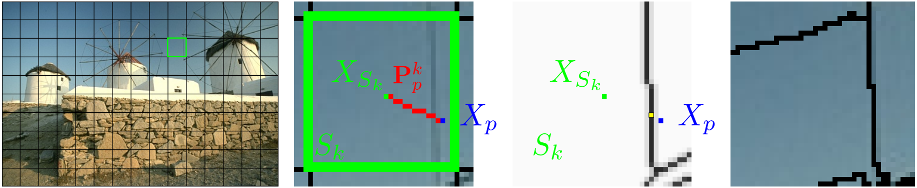

Image (itér. $\#0$) | Linear path | Max. contour | Result

Color distance on the neighborhood $V(p)$:

$$d_{\text{neigh.}}(V(p), S_k) = \sum_{q \in V(p)} d_{\text{color}}(F_q, F_{S_k}) w_{p,q}$$

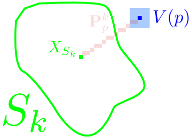

Color distance on the neighborhood $V(p)$:

$$d_{\text{neigh.}}(V(p), S_k) = \sum_{q \in V(p)} d_{\text{color}}(F_q, F_{S_k}) w_{p,q}$$

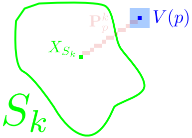

→ Robustness to noise.


Image

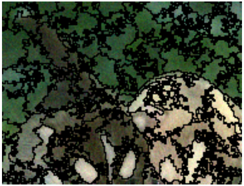
Without neighborhood


With neighborhood

Color distance on the neighborhood $V(p)$:

$$d_{\text{neigh.}}(V(p), S_k) = \sum_{q \in V(p)} d_{\text{color}}(F_q, F_{S_k}) w_{p,q}$$

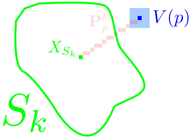

$\rightarrow$ Robustness to noise.

Image

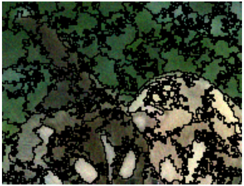

Without neighborhood

With neighborhood

Final SLIC distance [Achanta et al., 2012]:

$$D(p, S_k) = d_{\text{color}}(F_p, F_{S_k}) + d_{\text{spatial}}(X_p, X_{S_k})m$$

Color distance on the neighborhood $V(p)$:

$$d_{\text{neigh.}}(V(p), S_k) = \sum_{q \in V(p)} d_{\text{color}}(F_q, F_{S_k}) w_{p,q}$$

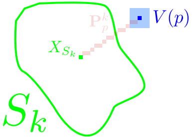

→ Robustness to noise.

Image

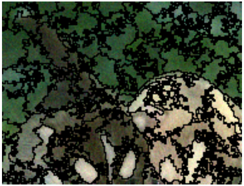

Without neighborhood

With neighborhood

Final distance SCALP:

$$D(p, S_k) = \left(d_{\text{neigh.}}(V(p), S_k) + d_{\text{path}}(\mathbf{P}_p^k, S_k) + d_{\text{spatial}}(p, S_k) m\right)\left(1 + d_{\text{contour}}(\mathbf{P}_p^k)\right)$$

Results - Qualitative comparison to state-of-the-art

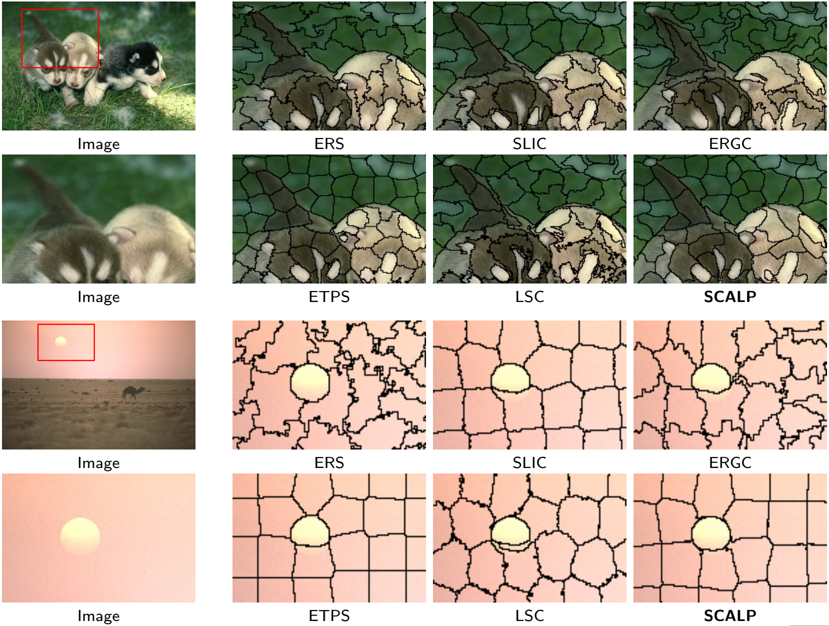

Results - Quantitative comparison to state-of-the-art

- Respect of image objects:

Image

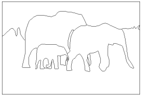

Manual segmentation

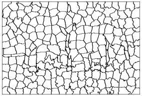

Superpixels

  - Achievable Segmentation Accuracy (ASA) [Liu et al., 2011]
    Superposition with the objects of the manual segmentation
  - F-measure (F) [Martin et al., 2004]
    Contour detection (Precision-Recall curves)

Results - Quantitative comparison to state-of-the-art

- Respect of image objects:


Image

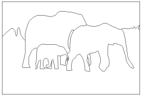
Manual segmentation

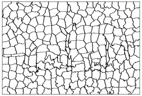
Superpixels

  - Achievable Segmentation Accuracy (ASA) [Liu et al., 2011]
    Superposition with the objects of the manual segmentation
  - F-measure (F) [Martin et al., 2004]
    Contour detection (Precision-Recall curves)

Validation on the BSD dataset: 200 images (321×481 pixels) [Martin et al., 2001]

Method	F	ASA
ERS [Liu et al., 2011]	0.593	0.951
SLIC [Achanta et al., 2012]	0.633	0.944
ERGC [Buyssens et al., 2014]	0.593	0.948
ETPS [Yao et al., 2015]	0.631	0.943
LSC [Chen et al., 2017]	0.607	0.950
SCALP	**0.680**	**0.954**

- Respect of image objects:


Image

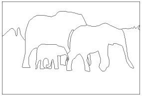
Manual segmentation

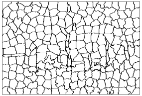
Superpixels

  - Achievable Segmentation Accuracy (ASA) [Liu et al., 2011]
    Superposition with the objects of the manual segmentation
  - F-measure (F) [Martin et al., 2004]
    Contour detection (Precision-Recall curves)

Validation on the BSD dataset: 200 images (321×481 pixels) [Martin et al., 2001]

Method	F	ASA
ERS [Liu et al., 2011]	0.593	0.951
SLIC [Achanta et al., 2012]	0.633	0.944
ERGC [Buyssens et al., 2014]	0.593	0.948
ETPS [Yao et al., 2015]	0.631	0.943
LSC [Chen et al., 2017]	0.607	0.950
SCALP	**0.680**	**0.954**

- Regularity of the decomposition:
  - Circularity (C) [Schick et al., 2012] $\rightarrow$ Limited evaluation metric

Evaluation of regularity - Shape regularity

Reference measures in the literature:

Circularity (C) [Schick et al., 2012]:

$$\mathsf{C}(S) = \frac{4\pi|S|}{|P(S)|^2}$$

Evaluation of regularity - Shape regularity

Reference measures in the literature:

Circularity (C) [Schick et al., 2012]:

$$\mathsf{C}(S) = \frac{4\pi|S|}{|P(S)|^2}$$

	Regular shapes		Standard shapes	
	Square	*Circle*	*Ellipse*	*Bean*

C	0.830	1.000	0.870	0.580

→ Low measure for the square

→ No robustness to noise

→ No robustness to scale

Reference measures in the literature:

Circularity (C) [Schick et al., 2012]:

$$\mathsf{C}(S) = \frac{4\pi|S|}{|P(S)|^2}$$

	Regular shapes		Standard shapes	
	Square	*Circle*	*Ellipse*	*Bean*

C	0.830	1.000	0.870	0.580

C	0.480	0.430	0.410	0.440

$\rightarrow$ Low measure for the square
$\rightarrow$ No robustness to noise
$\rightarrow$ No robustness to scale

Reference measures in the literature:

Circularity (C) [Schick et al., 2012]:

$$\mathsf{C}(S) = \frac{4\pi|S|}{|P(S)|^2}$$

	Regular shapes		Standard shapes	
	Square	*Circle*	*Ellipse*	*Bean*
C	0.830	1.000	0.870	0.580
C	0.480	0.430	0.410	0.440

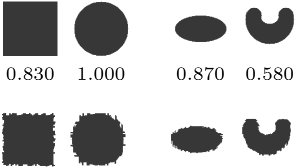

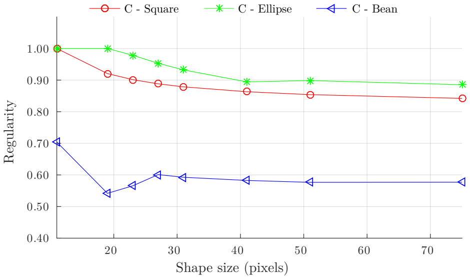

→ Low measure for the square
→ No robustness to noise
→ No robustness to scale

Definition: a regular shape should be convex

Shape Regularity Criteria (SRC):

$$\text{SRC}(S) = \frac{|S|}{|H_S|}$$

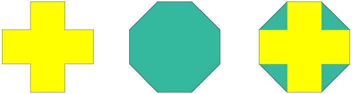
Shape S Convex hull H_S Superposition

Definition: a regular shape should be convex, with smooth contours

Shape Regularity Criteria (SRC):

$$\text{SRC}(S) = \frac{|S|}{|H_S|} . \frac{|\text{P}(H_S)|}{|\text{P}(S)|}$$

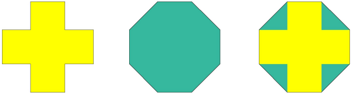

Shape S Convex hull H_S Superposition

Definition: a regular shape should be convex, with smooth contours and balanced.

Shape Regularity Criteria (SRC):

$$\mathsf{SRC}(S) = \frac{|S|}{|H_S|} \cdot \frac{|\mathsf{P}(H_S)|}{|\mathsf{P}(S)|} \cdot \frac{\min(\sigma_x, \sigma_y)}{\max(\sigma_x, \sigma_y)}$$

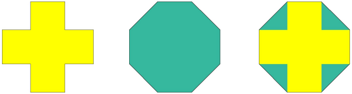

Shape S Convex hull H_S Superposition

Definition: a regular shape should be convex, with smooth contours and balanced.

Shape Regularity Criteria (SRC):

$$\text{SRC}(S) = \frac{|S|}{|H_S|} \cdot \frac{|\text{P}(H_S)|}{|\text{P}(S)|} \cdot \frac{\min(\sigma_x, \sigma_y)}{\max(\sigma_x, \sigma_y)}$$

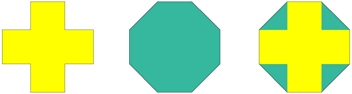

Shape S — Convex hull H_S — Superposition

	Regular shapes		Standard shapes	
	Square	*Circle*	*Ellipse*	*Bean*

	Square	*Circle*	*Ellipse*	*Bean*
C	0.830	1.000	0.870	0.580
SRC	**1.000**	**0.989**	**0.712**	**0.564**

→ Equivalent measure for the square and circle

→ Less sensitive to noise

→ Robust to scale

Definition: a regular shape should be convex, with smooth contours and balanced.

Shape Regularity Criteria (SRC):

$$\text{SRC}(S) = \frac{|S|}{|H_S|} \cdot \frac{|\mathsf{P}(H_S)|}{|\mathsf{P}(S)|} \cdot \frac{\min(\sigma_x, \sigma_y)}{\max(\sigma_x, \sigma_y)}$$

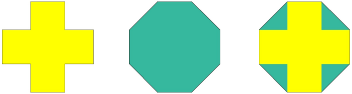

Shape S Convex hull H_S Superposition

	Regular shapes		Standard shapes	
	Square	*Circle*	*Ellipse*	*Bean*

C	0.830	1.000	0.870	0.580
SRC	**1.000**	**0.989**	**0.712**	**0.564**

C	0.480	0.430	0.410	0.440
SRC	**0.716**	**0.633**	**0.474**	**0.500**

→ Equivalent measure for the square and circle

→ Less sensitive to noise

→ Robust to scale

Definition: a regular shape should be convex, with smooth contours and balanced.

Shape Regularity Criteria (SRC):

$$\text{SRC}(S) = \frac{|S|}{|H_S|} \cdot \frac{|\text{P}(H_S)|}{|\text{P}(S)|} \cdot \frac{\min(\sigma_x, \sigma_y)}{\max(\sigma_x, \sigma_y)}$$

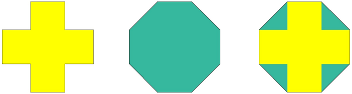

Shape S — Convex hull H_S — Superposition

	Regular shapes		Standard shapes	
	Square	*Circle*	*Ellipse*	*Bean*
				
C	0.830	1.000	0.870	0.580
SRC	**1.000**	**0.989**	**0.712**	**0.564**
				
C	0.480	0.430	0.410	0.440
SRC	**0.716**	**0.633**	**0.474**	**0.500**

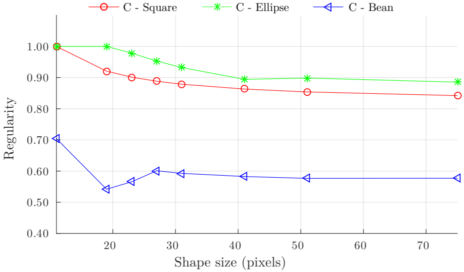

→ Equivalent measure for the square and circle

→ Less sensitive to noise

→ Robust to scale

Definition: a regular shape should be convex, with smooth contours and balanced.

Shape Regularity Criteria (SRC):

$$\text{SRC}(S) = \frac{|S|}{|H_S|} \cdot \frac{|\text{P}(H_S)|}{|\text{P}(S)|} \cdot \frac{\min(\sigma_x, \sigma_y)}{\max(\sigma_x, \sigma_y)}$$

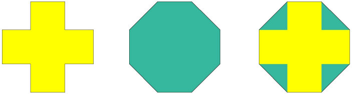

Shape S — Convex hull H_S — Superposition

	Regular shapes		Standard shapes	
	Square	*Circle*	*Ellipse*	*Bean*
				
C	0.830	1.000	0.870	0.580
SRC	**1.000**	**0.989**	**0.712**	**0.564**
				
C	0.480	0.430	0.410	0.440
SRC	**0.716**	**0.633**	**0.474**	**0.500**

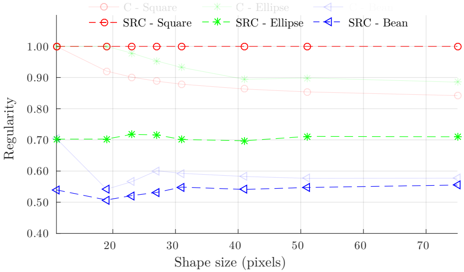

→ Equivalent measure for the square and circle

→ Less sensitive to noise

→ Robust to scale

Evaluation of regularity - Shape consistency

- Insufficient local evaluation

  $\rightarrow$ No taking into account of the consistency of shapes and sizes.

SRC $= 1.000$

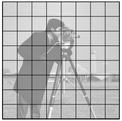

SRC $= 1.000$

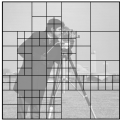

Evaluation of regularity - Shape consistency

- Insufficient local evaluation

  $\rightarrow$ No taking into account of the consistency of shapes and sizes.

SRC $= 1.000$

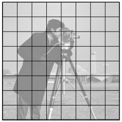

SRC $= 1.000$

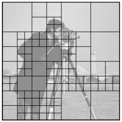

- Evaluation of the superpixel shape consistency

Smooth Matching Factor (SMF):

$$\text{SMF}(\mathcal{S}) = 1 - \sum_{S_k \in \mathcal{S}} \frac{|S_k|}{|I|} \cdot \left\| \frac{S_k^*}{|S_k^*|} - \frac{S^*}{|S^*|} \right\|_1 /2$$

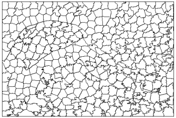

Decomposition $\mathcal{S}=\{S_k\}$

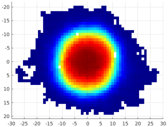

Average shape S^*

- Insufficient local evaluation

  $\rightarrow$ No taking into account of the consistency of shapes and sizes.

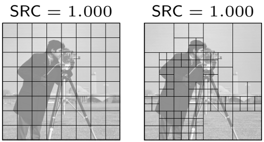

- Evaluation of the superpixel shape consistency

Smooth Matching Factor (SMF):

$$\text{SMF}(\mathcal{S}) = 1 - \sum_{S_k \in \mathcal{S}} \frac{|S_k|}{|I|} . \left\| \frac{S_k^*}{|S_k^*|} - \frac{S^*}{|S^*|} \right\|_1 /2$$

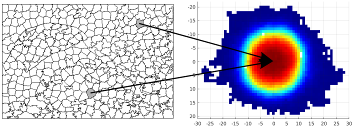

Decomposition $\mathcal{S}=\{S_k\}$ Average shape S^*

- Insufficient local evaluation

  → No taking into account of the consistency of shapes and sizes.

SRC $= 1.000$ SRC $= 1.000$

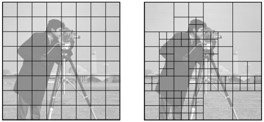

SMF $= 1.000$ SMF $= 0.498$

- Evaluation of the superpixel shape consistency

Smooth Matching Factor (SMF):

$$\text{SMF}(\mathcal{S}) = 1 - \sum_{S_k \in \mathcal{S}} \frac{|S_k|}{|I|} . \left\| \frac{S_k^*}{|S_k^*|} - \frac{S^*}{|S^*|} \right\|_1 /2$$

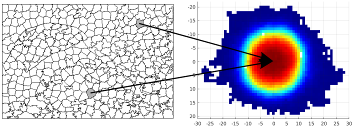

Decomposition $\mathcal{S}=\{S_k\}$ Average shape S^*

Evaluation of regularity - Shape consistency

- Insufficient local evaluation

  → No taking into account of the consistency of shapes and sizes.

SRC $= 1.000$ SRC $= 1.000$

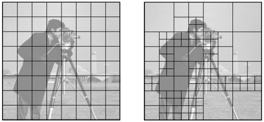

SMF $= 1.000$ SMF $= 0.498$

- Evaluation of the superpixel shape consistency

Smooth Matching Factor (SMF):

$$\text{SMF}(\mathcal{S}) = 1 - \sum_{S_k \in \mathcal{S}} \frac{|S_k|}{|I|} . \left\| \frac{S_k^*}{|S_k^*|} - \frac{S^*}{|S^*|} \right\|_1 /2$$

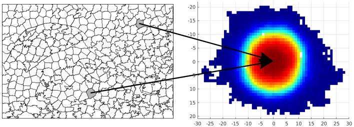

Decomposition $\mathcal{S}=\{S_k\}$ Average shape S^*

- Global evaluation of regularity

Global Regularity (GR):

$$\text{GR}(\mathcal{S}) = \text{SMF}(\mathcal{S}) \sum_{S_k \in \mathcal{S}} \frac{|S_k|}{|I|} \text{SRC}(S_k)$$

Validation on the standard BSD dataset [Martin et al., 2001].
200 images (321×481 pixels) with manual segmentations.

- Respect of image objects
  - Superposition with several objects: ASA
  - Contour detection: F-measure
- Regularity of the decomposition
  - Regularity of shape and consistency: GR

Method	F	ASA	GR
ERS [Liu et al., 2011]	0.593	0.951	0.195
SLIC [Achanta et al., 2012]	0.633	0.944	0.336
ERGC [Buyssens et al., 2014]	0.593	0.948	0.235
ETPS [Yao et al., 2015]	0.631	0.943	**0.494**
LSC [Chen et al., 2017]	0.607	0.950	0.238
SCALP	**0.680**	**0.954**	0.391

- Exemplar-based labeling: (SuperPatchMatch)

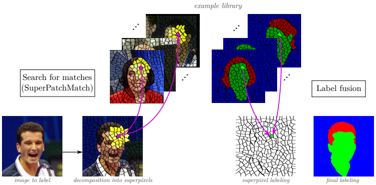

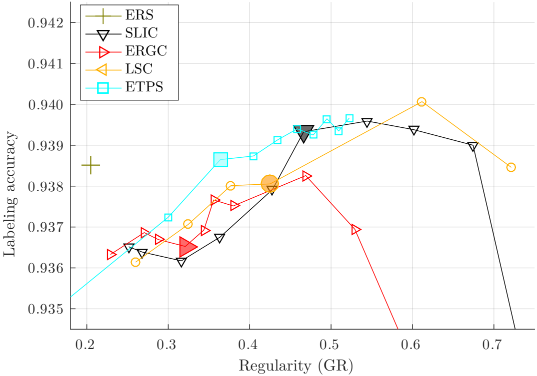

- Exemplar-based labeling: (SuperPatchMatch)

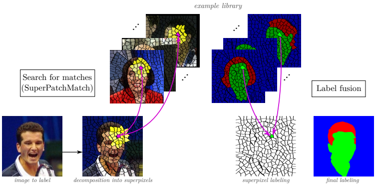

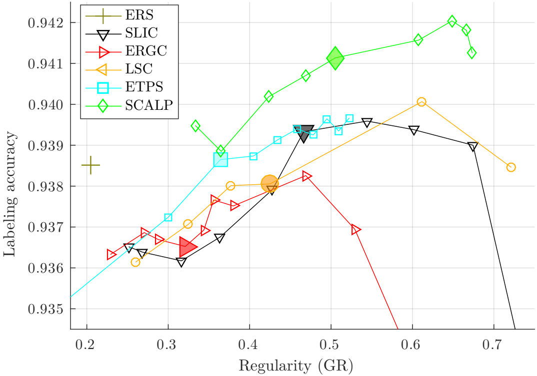

- State-of-the-art results with high regularity
- Limited computational time
- Natural extension to supervoxels

Associated publications:

- Rémi Giraud, Vinh-Thong Ta, and Nicolas Papadakis.
  SCALP: Superpixels with contour adherence using linear path.
  Proc. of International Conference on Pattern Recognition (ICPR), pages 2374–2379, 2016.
- Rémi Giraud, Vinh-Thong Ta, and Nicolas Papadakis.
  Décomposition en superpixels via l'utilisation de chemin linéaire.
  Actes du Groupe d'Études du Traitement du Signal et des Images (GRETSI), 2017.
- Rémi Giraud, Vinh-Thong Ta, and Nicolas Papadakis.
  Robust shape regularity criteria for superpixel evaluation.
  Proc. of IEEE International Conference on Image Processing (ICIP), 2017.
- Rémi Giraud, Vinh-Thong Ta, and Nicolas Papadakis.
  Evaluation framework of superpixel methods with a global regularity measure.
  Journal of Electronic Imaging (JEI), 2017.
- Rémi Giraud, Vinh-Thong Ta, and Nicolas Papadakis.
  Robust superpixels using color and contour features along linear path.
  Computer Vision and Image Understanding (CVIU) (en révision), 2017.

Conclusion

- Context:

  Non-local exemplar-based methods

  — without learning

  — large example datasets

  — fast

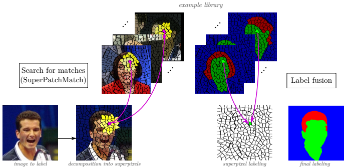

- Synthesis of contributions:

  1) Low resolution descriptors:

     → SCALP, GR, Superpatch

  2) Matching algorithms:

     → OPAL, SuperPatchMatch, SCT

  3) Applications:

     → 3D Medical image segmentation

     → Alzheimer's disease detection

     → Color transfer between images

     → Superpixel-based segmentation and labeling

     → ...

Perspectives

- Supervoxel-based segmentation of 3D medical images

  → To adapt SuperPatchMatch for complex structures, *e.g.*, tumors:

  — No prior on position

  — Contours correlated to the MRI image content

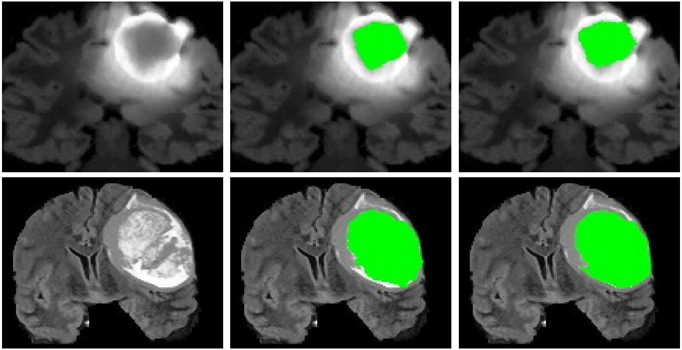

Image Ground truth SuperPatchMatch

Example of 2D segmentation of tumors on the BRATS dataset [Menze et al., 2015]

- Computer graphics (style transfer):

→ Important computational time
→ Copy of the same parts
→ Strict respect of contours

Target image

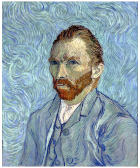

Source image

Patch-based
[Frigo et al., 2016]

- Computer graphics (style transfer):

$\rightarrow$ Important computational time
$\rightarrow$ Copy of the same parts
$\rightarrow$ Strict respect of contours


Target image

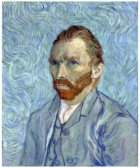
Source image


Patch-based
[Frigo et al., 2016]

Perspectives

- Computer graphics (style transfer):

$\rightarrow$ Important computational time
$\rightarrow$ Copy of the same parts
$\rightarrow$ Strict respect of contours

Target image

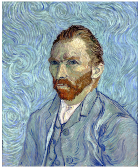

Source image

Patch-based
[Frigo et al., 2016]

$\rightarrow$ Superpixels to reduce the computational cost
$\rightarrow$ Constraint search for matches (SCT)
$\rightarrow$ To force the capture of the image contours

Image

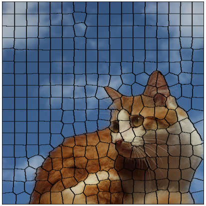

SCALP

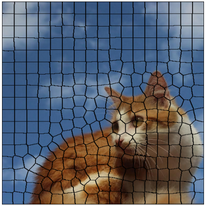

inversed SCALP

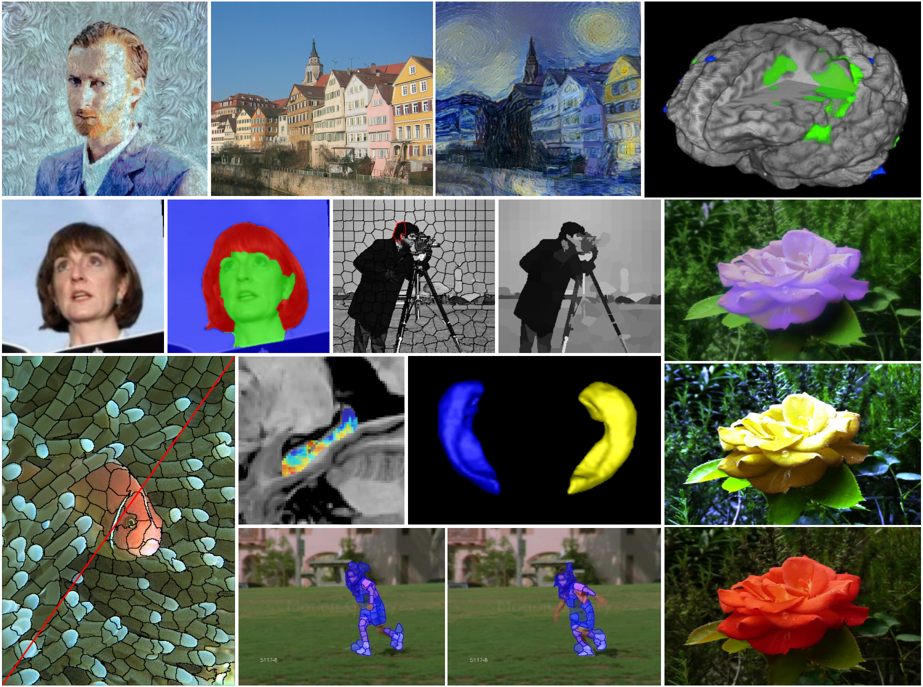
5117-8
5117-8

Matching algorithms and superpixels
for image analysis and processing

Thank you for your attention.

Questions?

Publications

- Vinh-Thong Ta, Rémi Giraud, D. Louis Collins, and Pierrick Coupé.
  Optimized PatchMatch for near real time and accurate label fusion.
  Proc. of Int. Conf. on Medical Image Computing and Computer-Assisted Intervention (MICCAI), pages 105–112, 2014.
- Rémi Giraud, Vinh-Thong Ta, Nicolas Papadakis, D. Louis Collins, and Pierrick Coupé.
  Optimisation de l'algorithme PatchMatch pour la segmentation de structures anatomiques.
  Actes du Groupe d'Études du Traitement du Signal et des Images (GRETSI), 2015.
- Rémi Giraud, Vinh-Thong Ta, Nicolas Papadakis, José V. Manjón, D. Louis Collins, and Pierrick Coupé.
  An optimized PatchMatch for multi-scale and multi-feature label fusion.
  NeuroImage (NIMG), 124:770–782, 2016.
- Rémi Giraud, Vinh-Thong Ta, and Nicolas Papadakis.
  SCALP: Superpixels with contour adherence using linear path.
  Proc. of International Conference on Pattern Recognition (ICPR), pages 2374–2379, 2016.
- Kilian Hett, Vinh-Thong Ta, Rémi Giraud, Mary Mondino, José V. Manjón, and Pierrick Coupé.
  Patch-based DTI grading: Application to alzheimer's disease classification.
  Proc. of Int. Work. on Patch-based Techniques in Medical Imaging (Patch-MI, MICCAI), pages 76–83, 2016.
- José V. Manjón, Pierrick Coupé, Jose E Romero, Vinh-Thong Ta, and Rémi Giraud.
  Ceres: A new cerebellum lobule segmentation method.
  Dépot logiciel : IDDN.FR.001.470008.000.S.P.2015.000.21000, 2016.
- Jose E Romero, Pierrick Coupé, Rémi Giraud, Vinh-Thong Ta, Vladimir Fonov, and Min Tae M Park, et al.
  CERES: A new cerebellum lobule segmentation method.
  NeuroImage (NIMG), 147:916–924, 2017.
- Rémi Giraud, Vinh-Thong Ta, and Nicolas Papadakis.
  Décomposition en superpixels via l'utilisation de chemin linéaire.
  Actes du Groupe d'Études du Traitement du Signal et des Images (GRETSI), 2017.

Publications

- Rémi Giraud, Vinh-Thong Ta, and Nicolas Papadakis.
  Transfert de couleurs basé superpixels.
  Actes du Groupe d'Études du Traitement du Signal et des Images (GRETSI), 2017.

- Rémi Giraud, Vinh-Thong Ta, and Nicolas Papadakis.
  Superpixel-based color transfer.
  Proc. of IEEE International Conference on Image Processing (ICIP), 2017.

- Rémi Giraud, Vinh-Thong Ta, and Nicolas Papadakis.
  Robust shape regularity criteria for superpixel evaluation.
  Proc. of IEEE International Conference on Image Processing (ICIP), 2017.

- Rémi Giraud, Vinh-Thong Ta, and Nicolas Papadakis.
  Evaluation framework of superpixel methods with a global regularity measure.
  Journal of Electronic Imaging (JEI), 2017.

- Rémi Giraud, Vinh-Thong Ta, Aurélie Bugeau, Pierrick Coupé, and Nicolas Papadakis.
  SuperPatchMatch: An algorithm for robust correspondences using superpixel patches.
  IEEE Trans. on Image Processing (TIP), 2017.

- Rémi Giraud, Vinh-Thong Ta, and Nicolas Papadakis.
  Robust superpixels using color and contour features along linear path.
  Computer Vision and Image Understanding (CVIU) (en révision), 2017.

References

- Achanta, R., Shaji, A., Smith, K., Lucchi, A., Fua, P., and Süsstrunk, S. (2012).
  SLIC superpixels compared to state-of-the-art superpixel methods.
  IEEE Trans. on Pattern Analysis and Machine Intelligence (PAMI), 34(11):2274–2282.
- Arbelaez, P., Maire, M., Fowlkes, C., and Malik, J. (2009).
  From contours to regions: An empirical evaluation.
  In *Proc. of IEEE Conf. on Computer Vision and Pattern Recognition (CVPR)*, pages 2294–2301.
- Barnes, C., Shechtman, E., Finkelstein, A., and Goldman, D. B. (2009).
  PatchMatch: A randomized correspondence algorithm for structural image editing.
  ACM Trans. on Graphics (ToG), 28(3).
- Benesova, W. and Kottman, M. (2014).
  Fast superpixel segmentation using morphological processing.
  In *Proc. of the Int. Conf. on Machine Vision and Machine Learning (MVML)*.
- Boccardi, M., Bocchetta, M., Apostolova, L. G., Barnes, J., Bartzokis, G., Corbetta, G., DeCarli, C., Firbank, M., Ganzola, R., and Gerritsen, L. (2014).
  Delphi definition of the EADC-ADNI Harmonized Protocol for hippocampal segmentation on magnetic resonance.
  Alzheimer's & Dementia, 11(2):126–138.
- Bresenham, J. E. (1965).
  Algorithm for computer control of a digital plotter.
  IBM Systems Journal, 4(1):25–30.
- Buades, A., Coll, B., and Morel, J.-M. (2005).
  A non-local algorithm for image denoising.
  In *Proc. of IEEE Conf. on Computer Vision and Pattern Recognition (CVPR)*, volume 2, pages 60–65.
- Buyssens, P., Gardin, I., Ruan, S., and Elmoataz, A. (2014).
  Eikonal-based region growing for efficient clustering.
  Image and Vision Computing, 32(12):1045–1054.

- Chang, J., Wei, D., and Fisher, J. W. (2013).
  A video representation using temporal superpixels.
  In *Proc. of IEEE Conf. on Computer Vision and Pattern Recognition (CVPR)*, pages 2051–2058.

- Chen, J., Li, Z., and Huang, B. (2017).
  Linear spectral clustering superpixel.
  IEEE Trans. on Image Processing (TIP).

- Collins, D., Holmes, C., Peters, T., and Evans, A. (1995).
  Automatic 3-D model-based neuroanatomical segmentation.
  Human Brain Mapping (HBM), 3(3):190–208.

- Collins, D. and Pruessner, J. (2010).
  Towards accurate, automatic segmentation of the hippocampus and amygdala from MRI by augmenting ANIMAL with a template library and label fusion.
  NeuroImage (NIMG), 52(4):1355–1366.

- Coupé, ., Manjón, J. V., Fonov, V., Pruessner, J., Robles, M., and Collins, D. (2011).
  Patch-based segmentation using expert priors: Application to hippocampus and ventricle segmentation.
  NeuroImage (NIMG), 54(2):940–954.

- Dollár, P. and Zitnick, L. (2013).
  Structured forests for fast edge detection.
  In *Proc. of IEEE International Conference on Computer Vision (ICCV)*, pages 1841–1848.

- Fortun, D., Bouthemy, P., and Kervrann, C. (2016).
  A variational aggregation framework for patch-based optical flow estimation.
  Journal of Mathematical Imaging and Vision (JMIV), 56(2):280–299.

- Frigo, O., Sabater, N., Delon, J., and Hellier, P. (2016).
  Split and match: Example-based adaptive patch sampling for unsupervised style transfer.
  In *Proc. of IEEE Conf. on Computer Vision and Pattern Recognition (CVPR)*, pages 553–561.

References

- Frigo, O., Sabater, N., Demoulin, V., and Hellier, P. (2014).
  Optimal transportation for example-guided color transfer.
  In *Proc. of Asian Conference on Computer Vision (ACCV)*, volume 9005, pages 655–670.
- Gatys, L. A., Ecker, A. S., and Bethge, M. (2015).
  A neural algorithm of artistic style.
  arXiv preprint arXiv:1508.06576.
- Gray, K. R., Austin, M., Wolz, R., McLeish, K., Boccardi, M., Frisoni, G., and Hill, D. (2014).
  Integration of EADC-ADNI Harmonised hippocampus labels into the LEAP automated segmentation technique.
  Alzheimer's & Dementia, 10:555.
- Heckemann, R. A., Hajnal, J. V., Aljabar, P., Rueckert, D., and Hammers, A. (2006).
  Automatic anatomical brain MRI segmentation combining label propagation and decision fusion.
  NeuroImage (NIMG), 33(1):115–126.
- Huang, G. B., Ramesh, M., Berg, T., and Learned-Miller, E. (2007).
  Labeled faces in the wild: A database for studying face recognition in unconstrained environments.
  Technical Report 07-49, University of Massachusetts, Amherst.
- Kae, A., Sohn, K., Lee, H., and Learned-Miller, E. (2013).
  Augmenting CRFs with Boltzmann machine shape priors for image labeling.
  In *Proc. of IEEE Conf. on Computer Vision and Pattern Recognition (CVPR)*, pages 2019–2026.
- Kim, M., Wu, G., Wang, Q., Lee, S.-W., and Shen, D. (2015).
  Improved image registration by sparse patch-based deformation estimation.
  NeuroImage (NIMG), 105:257–268.
- Korman, S. and Avidan, S. (2011).
  Coherency sensitive hashing.
  In *Proc. of IEEE International Conference on Computer Vision (ICCV)*, pages 1607–1614.

References

- Korman, S. and Avidan, S. (2016).
  Coherency sensitive hashing.
  IEEE Trans. on Pattern Analysis and Machine Intelligence (PAMI), 38(6):1099–1112.

- Liu, .-Y., Tuzel, O., Ramalingam, S., and Chellappa, R. (2011).
  Entropy rate superpixel segmentation.
  In *Proc. of IEEE Conf. on Computer Vision and Pattern Recognition (CVPR)*, pages 2097–2104.

- Liu, ., Yang, J., Huang, C., and Yang, M.-H. (2015).
  Multi-objective convolutional learning for face labeling.
  In *Proc. of IEEE Conf. on Computer Vision and Pattern Recognition (CVPR)*, pages 3451–3459.

- Liu, Y. (2013).
  Noise reduction by vector median filtering.
  Geophysics, 78(3):79–87.

- Machairas, V., Faessel, M., Cárdenas-Peña, D., Chabardes, T., Walter, T., and Decencière, E. (2015).
  Waterpixels.
  IEEE Trans. on Image Processing (TIP), 24(11):3707–3716.

- Maire, M., Arbelaez, P., Fowlkes, C., and Malik, J. (2008).
  Using contours to detect and localize junctions in natural images.
  In *Proc. of IEEE Conf. on Computer Vision and Pattern Recognition (CVPR)*, pages 1–8.

- Manjón, . V. and Coupé, P. (2016).
  volbrain: An online mri brain volumetry system.
  Frontiers in neuroinformatics, 10.

- Martin, D., Fowlkes, C., Tal, D., and Malik, J. (2001).
  A database of human segmented natural images and its application to evaluating segmentation algorithms and measuring ecological statistics.
  In *Proc. of IEEE International Conference on Computer Vision (ICCV)*, volume 2, pages 416–423.

References

- Martin, D. R., Fowlkes, C. C., and Malik, J. (2004).
  Learning to detect natural image boundaries using local brightness, color, and texture cues.
  IEEE Trans. on Pattern Analysis and Machine Intelligence (PAMI), 26(5):530–549.

- Mazziotta, J. C., Toga, A. W., Evans, A., Fox, P., and Lancaster, J. (1995).
  A probabilistic atlas of the human brain: Theory and rationale for its development.
  NeuroImage (NIMG), 2(2):89–101.

- Menze, B. H., Jakab, A., Bauer, S., Kalpathy-Cramer, J., Farahani, K., Kirby, J., Burren, Y., Porz, N., Slotboom, J., and Wiest, R. (2015).
  The multimodal brain tumor image segmentation benchmark (brats).
  IEEE Trans. on Medical Imaging (T-MI), 34(10):1993–2024.

- Moore, A. P., Prince, S. J., Warrell, J., Mohammed, U., and Jones, G. (2008).
  Superpixel lattices.
  In *Proc. of IEEE Conf. on Computer Vision and Pattern Recognition (CVPR)*, pages 1–8.

- Munkres, J. (1957).
  Algorithms for the assignment and transportation problems.
  SIAM Journal on Imaging Sciences (SIIMS), 5(1):32–38.

- Nguyen, R. M., Kim, S. J., and Brown, M. S. (2014).
  Illuminant aware gamut-based color transfer.
  In *Comput. Graph. Forum*, volume 33, pages 319–328.

- Pant, A., Rivest-Hénault, D., and Bourgeat, P. (2015).
  Efficient multi-scale patch-based segmentation.
  In *Proc. of Int. Work. on Patch-based Techniques in Medical Imaging (Patch-MI, MICCAI)*, pages 205–213.

- Park, M. T. M., Pipitone, J., Baer, L. H., Winterburn, J. L., Shah, Y., Chavez, S., Schira, M. M., Lobaugh, N. J., Lerch, J. P., Voineskos, A. N., et al. (2014).
  Derivation of high-resolution mri atlases of the human cerebellum at 3t and segmentation using multiple automatically generated templates.
  NeuroImage (NIMG), 95:217–231.

References

- Pitié, F., Kokaram, A. C., and Dahyot, R. (2007).
  Automated colour grading using colour distribution transfer.
  Computer Vision and Image Understanding (CVIU), 107(1–2):123–137.

- Rabin, J., Ferradans, S., and Papadakis, N. (2014).
  Adaptive color transfer with relaxed optimal transport.
  In *Proc. of IEEE International Conference on Image Processing (ICIP)*.

- Rabin, J., Peyré, G., Delon, J., and Bernot, M. (2012).
  Wasserstein barycenter and its application to texture mixing.
  In *International Conference on Scale Space and Variational Methods in Computer Vision*, pages 435–446.

- Reinhard, E., Adhikhmin, M., Gooch, B., and Shirley, P. (2001).
  Color transfer between images.
  IEEE Computer Graphics and Applications (CGA), 21(5):34–41.

- Ren, X. and Malik, J. (2003).
  Learning a classification model for segmentation.
  In *Proc. of IEEE International Conference on Computer Vision (ICCV)*, pages 10–17.

- Roche, F., Schaerer, J., Gouttard, S., Istace, A., Belaroussi, B., Yu, H. J., Bracoud, L., Pachai, C., and DeCarli, C. (2014).
  Accuracy of BMAS hippocampus segmentation using the harmonized hippocampal protocol.
  Alzheimer's & Dementia, 10(4):56.

- Rubio, A., Yu, L., Simo-Serra, E., and Moreno-Noguer, F. (2016).
  BASS: Boundary-aware superpixel segmentation.
  In *Proc. of International Conference on Pattern Recognition (ICPR)*.

- Schick, A., Fischer, M., and Stiefelhagen, R. (2012).
  Measuring and evaluating the compactness of superpixels.
  In *Proc. of International Conference on Pattern Recognition (ICPR)*, pages 930–934.

References

- Tai, Y.-W., Jia, J., and Tang, C.-K. (2005).
  Local color transfer via probabilistic segmentation by expectation-maximization.
  In *Proc. of IEEE Conf. on Computer Vision and Pattern Recognition (CVPR)*, pages 747–754.
- Tangaro, S., Amoroso, N., Boccardi, M., Bruno, S., Chincarini, A., Ferraro, G., Frisoni, G. B., Maglietta, R., and Redolfi, A. (2014).
  Automated voxel-by-voxel tissue classification for hippocampal segmentation: Methods and validation.
  Physica Medica, 30(8):878–887.
- Tong, ., Wolz, R., Coupé, P., Hajnal, J. V., and Rueckert, D. (2013).
  Segmentation of MR images via discriminative dictionary learning and sparse coding: Application to hippocampus labeling.
  NeuroImage (NIMG), 76:11–23.
- Tsai, D., Flagg, M., Nakazawa, A., and Rehg, J. M. (2012).
  Motion coherent tracking using multi-label mrf optimization.
  International Journal of Computer Vision (IJCV), 100(2):190–202.
- Van den Bergh, M., Boix, X., Roig, G., de Capitani, B., and Van Gool, L. (2012).
  SEEDS: Superpixels extracted via energy-driven sampling.
  In *Proc. of European Conference on Computer Vision (ECCV)*, pages 13–26.
- Weier, K., Fonov, V., Lavoie, K., Doyon, J., and Collins, D. (2014).
  Rapid automatic segmentation of the human cerebellum and its lobules (rascal)—implementation and application of the patch-based label-fusion technique with a template library to segment the human cerebellum.
  Human Brain Mapping (HBM), 35(10):5026–5039.
- Xiaofeng, R. and Bo, L. (2012).
  Discriminatively trained sparse code gradients for contour detection.
  In *Proc. of Int. Conf. on Neural Information Processing Systems (NIPS)*, pages 584–592.
- Yao, J., Boben, M., Fidler, S., and Urtasun, R. (2015).
  Real-time coarse-to-fine topologically preserving segmentation.
  In *Proc. of IEEE Conf. on Computer Vision and Pattern Recognition (CVPR)*, pages 2947–2955.

References

- Zhu, H., Cheng, H., Yang, X., and Fan, Y. (2017).
  Metric learning for multi-atlas based segmentation of hippocampus.
  International Journal of Computer Vision (IJCV), 15(1):41–50.

- Zijdenbos, A. P., Dawant, B. M., Margolin, R. A., and Palmer, A. C. (1994).
  Morphometric analysis of white matter lesions in MR images: method and validation.
  IEEE Trans. on Medical Imaging (T-MI), 13(4):716–724.

Annex

Matching algorithm based on patches for medical image segmentation

Reconstruction of an image A from the selected patches in an image B

Image A

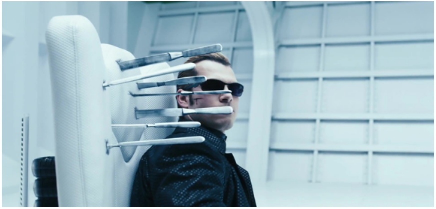

Image B

Image $\tilde{A}$ (exhaustive search) (t=10h)

Image $\tilde{A}$ [Barnes et al., 2009] (t=14s)

Coherency Sensitive Hashing [Korman and Avidan, 2011, Korman and Avidan, 2016]

Idea: To use a patch-based hash table to facilitate the search for matches.

→ Necessity to have the input image to compute the hashing of example images.

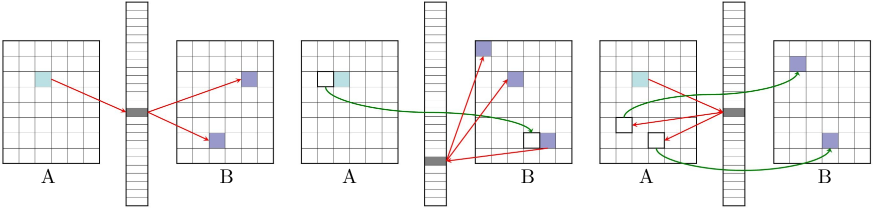

Direct access from the table　　Propagation + table　　Propagation from A

The OPAL method - Label fusion

S subject to segment,
$T = \{T_1, \ldots, T_n\}_{n=1,\ldots N}$ the N example models,
$P(\mathbf{x_i}) \in S$ the 3D patch at the position $\mathbf{x_i} = (x, y, z) \in S$,
$\mathcal{K}_i = \{\mathbf{x_{j,t}}\}$ the set of positions of selected patches,
$l(\mathbf{x_{j,t}})$ the label (0 or 1) given by the expert at voxel $\mathbf{x_{j,t}}$,

Label fusion:

$$\mathcal{L}(P(\mathbf{x_i})) = \frac{\sum\limits_{\mathbf{x_{j,t}} \in \mathcal{K}_i} \omega\left(\mathbf{x_i}, \mathbf{x_{j,t}}\right) L\left(P(\mathbf{x_{j,t}})\right)}{\sum\limits_{\mathbf{x_{j,t}} \in \mathcal{K}_i} \omega\left(\mathbf{x_i}, \mathbf{x_{j,t}}\right)} \qquad \mathcal{S}(\mathbf{x_i}) = \begin{cases} 1, & \text{if } \mathcal{L}(\mathbf{x_i}) \geq 0.5 \\ 0, & \text{otherwise} \end{cases}$$

Comparison of patches:

$$\omega(\mathbf{x_i}, \mathbf{x_{j,t}}) = \exp\left(1 - \left(\frac{\|P(\mathbf{x_i}) - P(\mathbf{x_{j,t}})\|_2^2}{h(\mathbf{x_i})^2} + \frac{\|\mathbf{x_i} - \mathbf{x_j}\|_2}{\sigma^2}\right)\right)$$

$$h(\mathbf{x_i})^2 = \alpha^2 \min_{\mathbf{x_{j,t}} \in \mathcal{K}_i} \left(\|P(\mathbf{x_i}) - P(\mathbf{x_{j,t}})\|_2^2 + \epsilon\right)$$

Impact of the initialization window size

$\rightarrow$ Set by default at $13{\times}13{\times}13$ voxels

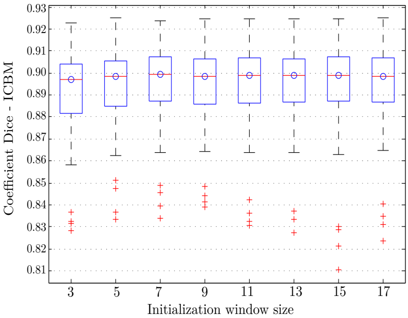

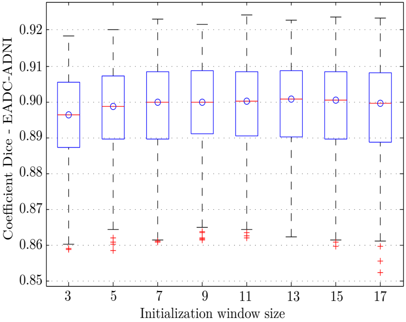

Very limited computational time

$\rightarrow$ Independent multi-feature and multi-scale search and fusion

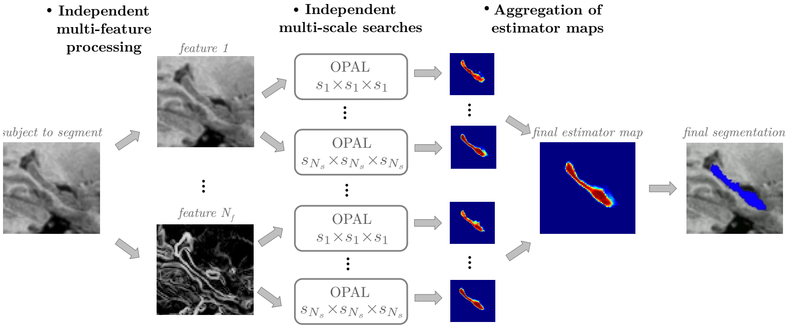

Dataset	Multi-feature	Multi-scale	Median Dice	Average Dice	p-value	Computational time
ICBM	✗	✗	89.4%	$89.1 \pm 1.85\%$	$< 10^{-14}$	$0.27s$
	✓	✗	89.8%	$89.6 \pm 1.68\%$	0.0131	$0.53s$
	✓	✓	89.9%	$89.7 \pm 1.70\%$	$\times$	$0.92s$
EADC-ADNI	✗	✗	89.4%	$89.2 \pm 1.55\%$	$< 10^{-25}$	$0.49s$
	✓	✗	89.7%	$89.6 \pm 1.45\%$	$< 10^{-8}$	$0.95s$
	✓	✓	90.1%	$89.8 \pm 1.46\%$	$\times$	$1.48s$

The OPAL method - Impact of parameters

Very limited computational time
 → Independent multi-feature and multi-scale search and fusion

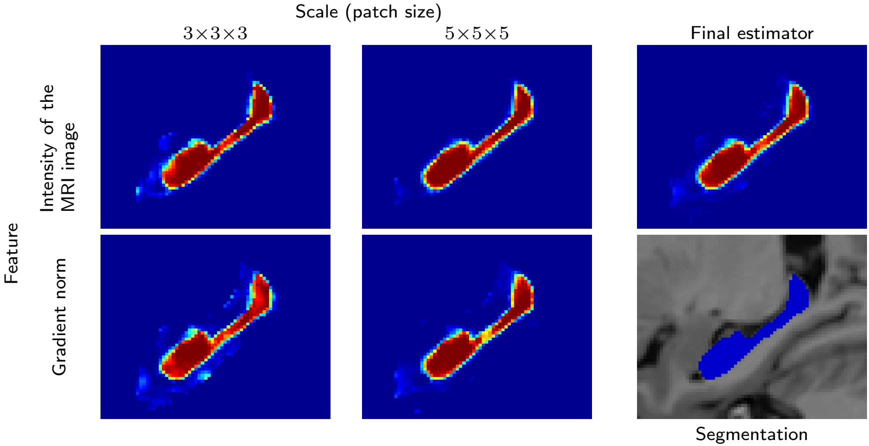

The OPAL method - Impact of parameters

Very limited computational time

$\rightarrow$ Independent multi-feature and multi-scale search and fusion

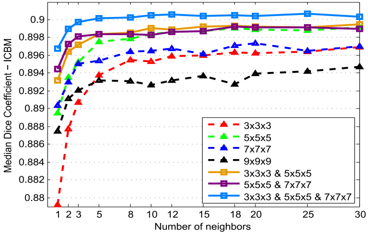

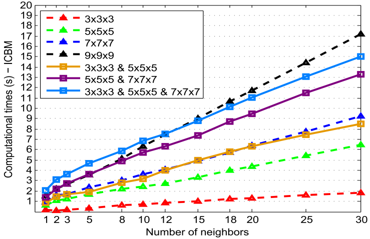

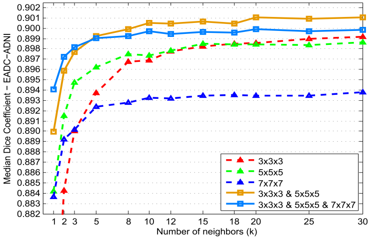

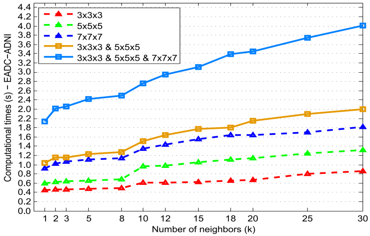

The OPAL method - Results

Validation metric [Zijdenbos et al., 1994]:

$$\text{Dice}(\mathcal{S}_{\text{expert}}, \mathcal{S}_{\text{auto}}) = \frac{2|\mathcal{S}_{\text{expert}} \cap \mathcal{S}_{\text{auto}}|}{|\mathcal{S}_{\text{expert}}| + |\mathcal{S}_{\text{auto}}|}$$

- ICBM dataset: 80 young healthy subjects [Mazziotta et al., 1995]
  Inter-expert variability: 90%.

Method	Median Dice	Computational time
Patch-based [Coupé et al., 2011]	$88.2 \pm 2.19\%$	$(\times 700)$
Multi-templates [Collins and Pruessner, 2010]	$88.6 \pm 2.05\%$	$(\times 4300)$
Sparse coding [Tong et al., 2013]	$88.7 \pm 1.94\%$	$(\times 6000)$
Dictionary learning [Tong et al., 2013]	$89.0 \pm 1.90\%$	$(\times 1000)$
OPAL (2015)	$\mathbf{90.0 \pm 1.70\%}$	$\mathbf{0.92s}$

- EADC-ADNI: 100 healthy and unhealthy subjects [Boccardi et al., 2014]
  Inter-expert variability: 89%.

Method	Average Dice	Computational time
Random Forest [Tangaro et al., 2014]	$76.0 \pm 7.00\%$	$\times$
Multi-templates [Roche et al., 2014]	$86.6 \pm 1.70\%$	$\times$
Multi-templates [Gray et al., 2014]	$87.6 \pm 2.07\%$	$\times$
Patch-based [Zhu et al., 2017]	$88.3 \pm 2.50\%$	$\times$
Multi-scale patch-based [Pant et al., 2015]	$89.2 \pm 2.22\%$	$(\times 200)$
OPAL (2015)	$\mathbf{89.8 \pm 1.46\%}$	$\mathbf{1.48s}$

The complexity of OPAL only depends on the subject size:
→ Adding automatically segmented subjects to the library

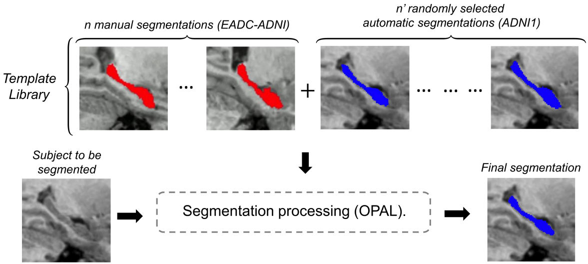

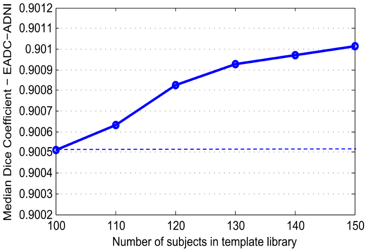

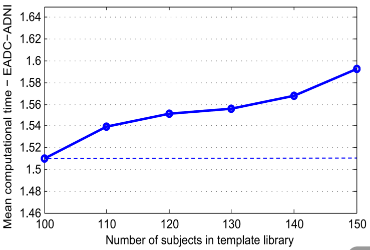

Several complex and adjacent structures
→ Weighting and regularization of estimator maps [Romero et al., 2017]

Comparison to MAGET [Park et al., 2014] and RASCAL [Weier et al., 2014]
Computational time: MAGET (2h), RASCAL (4h), CERES (1mn)

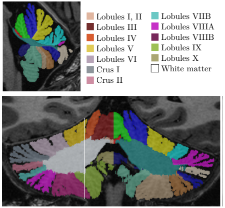

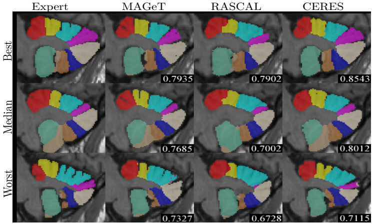

Structure	MAGeT	RASCAL	CERES	Intra-expert
Lobule I-II	0.3960 ± 0.1424	0.3260 ± 0.2178	**0.5201** ± 0.1555	0.639
Lobule III	0.6800 ± 0.1741	0.6379 ± 0.2165	**0.7213** ± 0.1572	0.751
Lobule IV	0.6980 ± 0.1440	0.6627 ± 0.1611	**0.7271** ± 0.1346	0.818
Lobule V	0.7320 ± 0.1398	0.6666 ± 0.1560	**0.7561** ± 0.1332	0.881
Lobule VI	**0.8710** ± 0.0359	0.7969 ± 0.0523	0.8695 ± 0.0316	0.912
Lobule Crus I	0.8870 ± 0.0257	0.8383 ± 0.0351	**0.9007** ± 0.0152	0.904
Lobule Crus II	0.7780 ± 0.0679	0.7340 ± 0.0667	**0.8096** ± 0.0569	0.900
Lobule VIIB	0.5990 ± 0.1487	0.5820 ± 0.1137	**0.6850** ± 0.1205	0.863
Lobule VIIIA	0.7300 ± 0.0934	0.6757 ± 0.1426	**0.7926** ± 0.0759	0.860
Lobule VIIIB	0.7970 ± 0.0607	0.7783 ± 0.0931	**0.8533** ± 0.0390	0.833
Lobule IX	0.8560 ± 0.0384	0.8460 ± 0.0545	**0.8849** ± 0.0327	0.874
Lobule X	0.7540 ± 0.0490	0.7237 ± 0.0680	**0.7548** ± 0.0469	0.760
Cerebellum	0.9250 ± 0.0094	0.9349 ± 0.0089	**0.9377** ± 0.0090	0.941
Average	0.7320 ± 0.0568	0.6890 ± 0.0524	**0.7729** ± 0.0427	0.833

Automatic classification using OPAL for the search of matches.
Label fusion of the pathologies of the library models.

(NC = Normal Controls, AD = Alzheimer Disease, MCI = Mild Cognitive Impairment)

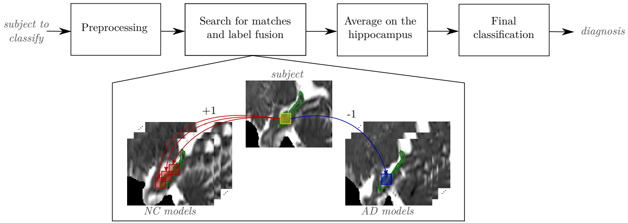

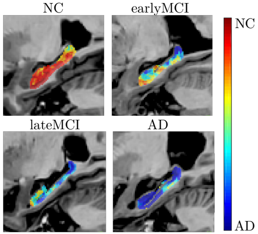

Classification performances on several features.

	Features	NC vs AD	NC vs MCI	AD vs MCI	eMCI vs lMCI
Average	Volume	88.4/83.1	69.5/63.9	71.1/67.2	67.2/63.7
	FA	64.2/59.2	57.7/56.1	54.0/52.7	38.2/43.1
	MD	85.7/80.3	66.0/62.6	75.0/72.5	67.6/62.8
	AxD	83.5/81.4	63.5/58.0	74.3/70.2	68.9/66.8
	RD	86.2/79.2	66.5/62.3	74.8/70.5	66.0/61.5
OPAL	T1	**93.4/87.8**	**71.3/64.1**	82.0/73.4	68.7/66.2
	FA	85.0/80.1	63.5/60.1	74.9/70.3	63.0/60.7
	MD	90.6/86.5	68.8/60.7	80.4/76.3	70.4/65.8
	AxD	91.1/85.8	68.7/59.6	80.2/73.1	**71.8/67.6**
	RD	90.3/85.1	68.9/61.0	**80.0/76.5**	69.3/65.4

The OPAL method - volBrain

Integration of OPAL to the volBrain platform [Manjón and Coupé, 2016] (http://volbrain.upv.es)

- Online volumetric study system of cerebral MRI images
- Detailed reports (tissues, white matter, hippocampus, etc.) with segmentation files
- Since mars 2015, more than 1400 users across the world for more than 45000 processed MRI images

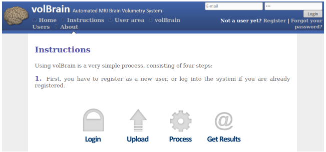

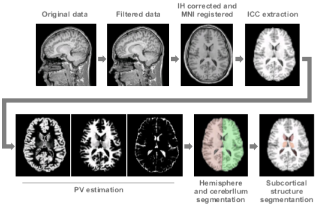

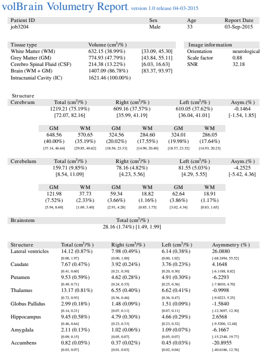

volBrain Volumetry Report. version 1.0 release 04-03-2015

Patient ID	Sex	Age	Report Date
job3204	Male	33	03-Sep-2015

Tissue type	Volume (cm³/%)	
White Matter (WM)	632.15 (38.99%)	[33.09, 45.30]
Grey Matter (GM)	774.93 (47.79%)	[43.84, 55.11]
Cerebro Spinal Fluid (CSF)	214.38 (13.22%)	[6.03, 16.63]
Brain (WM + GM)	1407.09 (86.78%)	[83.37, 93.97]
Intracranial Cavity (IC)	1621.46 (100.00%)	

Image information	
Orientation	neurological
Scale factor	0.88
SNR	32.18

Structure

Cerebrum	Total (cm³/%)	Right (cm³/%)	Left (cm³/%)	Asym.(%)
	1219.21 (75.19%) [72.07, 82.16]	609.16 (37.57%) [35.99, 41.19]	610.05 (37.62%) [36.04, 41.01]	-0.1464 [-1.54, 1.85]

GM	WM	GM	WM	GM	WM
648.56 (40.00%) [37.14, 46.64]	570.65 (35.19%) [29.85, 40.62]	324.56 (20.02%) [18.56, 23.33]	284.60 (17.55%) [14.90, 20.40]	324.01 (19.98%) [18.57, 23.32]	286.05 (17.64%) [14.93, 20.23]

Cerebelum	Total (cm³/%)	Right (cm³/%)	Left (cm³/%)	Asym.(%)
	159.71 (9.85%) [8.54, 11.09]	78.16 (4.82%) [4.23, 5.56]	81.55 (5.03%) [4.29, 5.55]	-4.2525 [-5.42, 4.36]

GM	WM	GM	WM	GM	WM
121.98 (7.52%) [5.94, 8.60]	37.73 (2.33%) [1.69, 3.40]	59.34 (3.66%) [2.91, 4.28]	18.82 (1.16%) [0.85, 1.75]	62.64 (3.86%) [3.02, 4.34]	18.91 (1.17%) [0.83, 1.65]

Brainstem	Total (cm³/%)
	28.16 (1.74%) [1.49, 1.99]

Structure	Total (cm³/%)	Right (cm³/%)	Left (cm³/%)	Asymmetry (%)
Lateral ventricles	14.12 (0.87%) [0.00, 1.97]	7.98 (0.49%) [0.00, 1.00]	6.14 (0.38%) [0.00, 1.02]	26.0880 [-68.2494, 55.52]
Caudate	7.67 (0.47%) [0.41, 0.60]	3.92 (0.24%) [0.21, 0.30]	3.76 (0.23%) [0.20, 0.30]	4.1648 [-6.1188, 8.82]
Putamen	9.53 (0.59%) [0.49, 0.71]	4.62 (0.28%) [0.24, 0.35]	4.91 (0.30%) [0.25, 0.36]	-6.2293 [-7.8010, 4.70]
Thalamus	13.17 (0.81%) [0.72, 0.93]	6.55 (0.40%) [0.36, 0.46]	6.62 (0.41%) [0.36, 0.47]	-0.9998 [-9.0223, 5.25]
Globus Pallidus	2.99 (0.18%) [0.14, 0.21]	1.48 (0.09%) [0.07, 0.11]	1.51 (0.09%) [0.07, 0.11]	-1.5840 [-12.3697, 12.30]
Hippocampus	9.45 (0.58%) [0.46, 0.64]	4.79 (0.30%) [0.23, 0.33]	4.66 (0.29%) [0.23, 0.32]	2.6568 [-9.5200, 12.48]
Amygdala	2.11 (0.13%) [0.09, 0.15]	1.02 (0.06%) [0.05, 0.07]	1.09 (0.07%) [0.05, 0.07]	-6.1667 [-15.2340, 19.77]
Accumbens	0.82 (0.05%) [0.03, 0.07]	0.37 (0.02%) [0.01, 0.03]	0.45 (0.03%) [0.02, 0.04]	-20.8955 [-40.6186, 12.76]

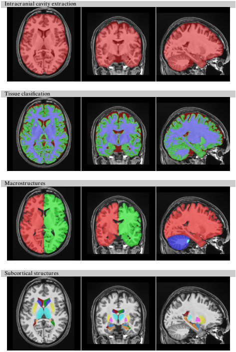

Annex

Matching algorithm based on patches of superpixels and applications

Adaptation of PatchMatch propagation step

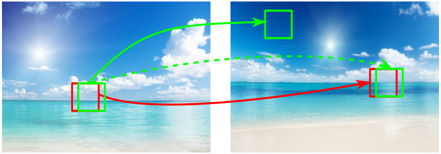

A B

Selection of the neighbor with the most similar orientation:

$$C_{(i')} = \operatorname*{argmin}_{k \in \mathcal{N}^{B}_{\mathcal{M}(i')}} \|(\theta_{ii'} + \pi) - \theta_{i'k}\|_1$$

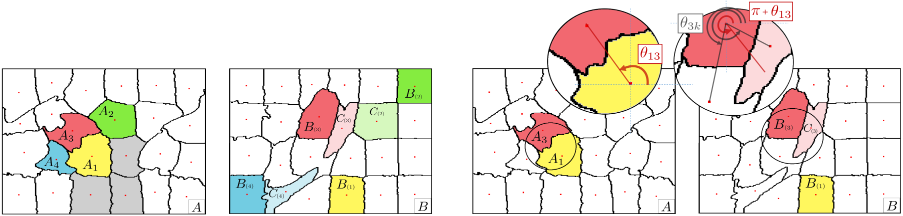

The SCT method - Previous works

Target image

Source image

- Parametric methods: statistics transfer.
  [Reinhard et al., 2001, Tai et al., 2005]

  → No guarantee to have a relevant color transfer.

- Optimal transport (OT): transfer of color histogram.
  [Pitié et al., 2007, Rabin et al., 2012, Frigo et al., 2014]

  → The exact transfer may lead to visual outliers.

- Relaxed OT: adaptive transfer of the source colors
  using superpixels. [Rabin et al., 2014]

  → High computational cost with OT methods.

[Reinhard et al., 2001]

[Pitié et al., 2007]

[Rabin et al., 2014]

Proposed solution: A superpixel in B cannot be selected more than ϵ times.

If a superpixel A_i finds a better match B_k already taken by ϵ superpixels A_j?

Switch between matches:

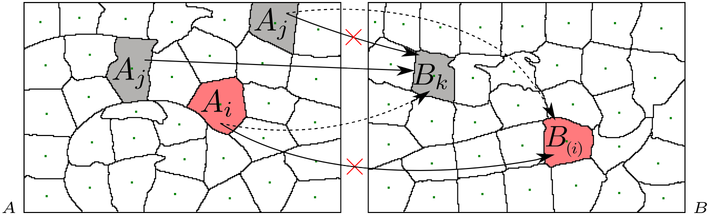

Switch illustration ($\epsilon = 2$)

$$C(A_i, A_j) = \big(D(A_i, B_k) - D(A_i, B_{(i)})\big) + \big(D(A_j, B_{(i)}) - D(A_j, B_k)\big)\,.$$

$$\text{If } \; \exists A_j, C(A_i, A_j) < 0 \quad \begin{cases} \underset{A_j}{\text{argmin}}\; C(A_i, A_j) \rightarrow B_{(i)}, \\ A_i \rightarrow B_k. \end{cases}$$

$\rightarrow$ Optimization of the total matching distance $\sum_i D(A_i, B_{(i)})$.

→ With the constraint set by ϵ, global selection of the source color palette.

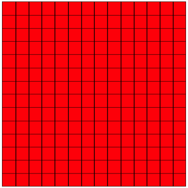
Target image

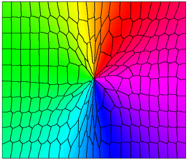
Source image

Without constraint ($\epsilon = \infty$)


Transfer result (average colors)


Selected superpixels

With constraint ($\epsilon = 1$)

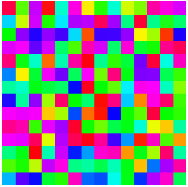
Transfer result (average colors)

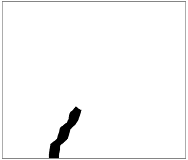
Selected superpixels

The SCT method - Global assignment problem

With $\epsilon = 1$, approximation of the optimal assignment problem:

"Given two sets $A=\{A_i\}_{i\in\{1,\ldots,|A|\}}$ and $B=\{B_j\}_{j\in\{1,\ldots,|B|\}}$ with $|A| \leq |B|$, association of each A_i to a unique $B_{(i)}$ that minimizes $\sum_i D(A_i, B_{(i)})$."

Problem addressed with costly optimal algorithms [Munkres, 1957]

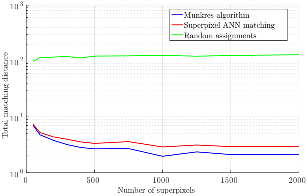

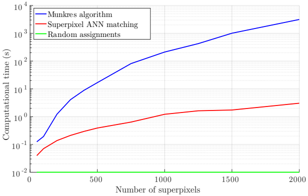

Selected colors

Target image A

$\widetilde{A}$ with [Munkres, 1957]

Source image B

$\widetilde{A}$ with constrained SPM

$\rightarrow$ Close results to the optimal resolution in very reduced computational time.

- Fusion of selected colors by non-local means [Buades et al., 2005]:

  Superpixel $A_i = [X_i, C_i] = [(x_i, y_i), (r_i, g_i, b_i)]$.

  For all pixels $p \in A_i$, contribution of superpixels A_j.

Color fusion:

$$A_t(p) = \frac{\sum_j \omega(p, A_j)\bar{C}_{B_{(j)}}}{\sum_j \omega(p, A_j)}$$

$\rightarrow$ Only transfer existing source colors.

- Weighting based on spatial and color similarity:

Distance using covariance information of A_i:

$$\omega(p, A_j) = \exp\left(-(p - \bar{A}_j)^T Q_i^{-1}(p - \bar{A}_j)\right)$$

$\rightarrow$ Respect of the target image structures.

The SCT method - Step summary

Total computational time < 1s (480×360 pixels).

Target image

Source image

< 0.2s

Superpixels

< 0.1s

Transfer of average colors

< 0.3s

Final result

With the constraint set by ϵ, homogeneous selection of the source superpixels.
$\rightarrow$ Global transfer of the source color palette.


Target image

SCT ($\epsilon = \infty$)

Transfer result

SCT ($\epsilon = 3$)

Transfer result


Source image


Selection map


Selection map

The SCT method - Influence of the matching constraint

With the constraint set by ϵ, homogeneous selection of the source superpixels.
$\rightarrow$ Global transfer of the source color palette.


Target image

SCT ($\epsilon = \infty$)


Transfer result

SCT ($\epsilon = 3$)


Transfer result


Source image


Selection map

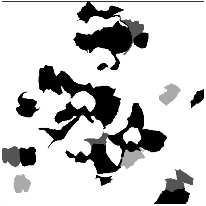
Selection map

The SCT method - Comparison to state-of-the-art

Comparison to:

- Optimal transport [Pitié et al., 2007]
- Relaxed optimal transport [Rabin et al., 2014]
- 3D color gamut mapping [Nguyen et al., 2014]

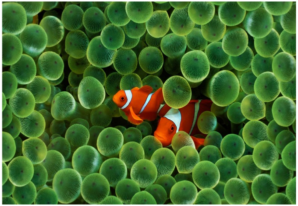

Target image

Source image

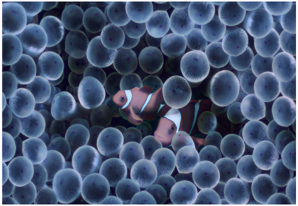

SCT

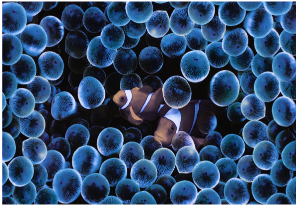

[Pitié et al., 2007]

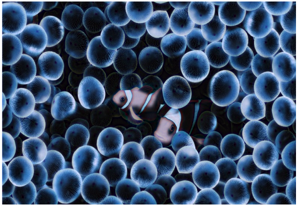

[Rabin et al., 2014]

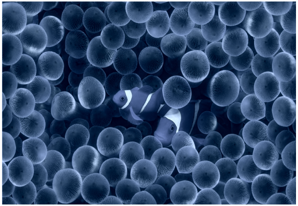

[Nguyen et al., 2014]

The SCT method - Comparison to state-of-the-art

Comparison to:

- Optimal transport [Pitié et al., 2007]
- Relaxed optimal transport [Rabin et al., 2014]
- 3D color gamut mapping [Nguyen et al., 2014]

Target image

Source image

SCT

[Pitié et al., 2007]

[Rabin et al., 2014]

[Nguyen et al., 2014]

Comparison to:
- Optimal transport [Pitié et al., 2007]
- Relaxed optimal transport [Rabin et al., 2014]
- 3D color gamut mapping [Nguyen et al., 2014]


Target image


Source image


SCT


[Pitié et al., 2007]


[Rabin et al., 2014]


[Nguyen et al., 2014]

The SCT method - Comparison to state-of-the-art

Comparison to:
- Optimal transport [Pitié et al., 2007]
- Relaxed optimal transport [Rabin et al., 2014]
- 3D color gamut mapping [Nguyen et al., 2014]

Target image

Source image

SCT

[Pitié et al., 2007]

[Rabin et al., 2014]

[Nguyen et al., 2014]

The SCT method - Comparison to state-of-the-art

Comparison to:

- Optimal transport [Pitié et al., 2007]
- Relaxed optimal transport [Rabin et al., 2014]
- 3D color gamut mapping [Nguyen et al., 2014]

Target image

Source image

SCT

[Pitié et al., 2007]

[Rabin et al., 2014]

[Nguyen et al., 2014]

The SCT method - Several source images

Target image

Source images

SCT

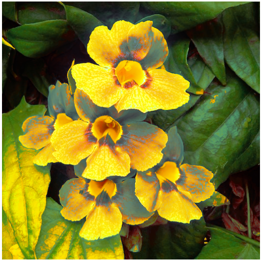

[Pitié et al., 2007]

[Rabin et al., 2014]

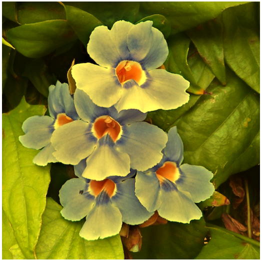

[Nguyen et al., 2014]

Displacements between the superpixel-based and superpatch-based matches

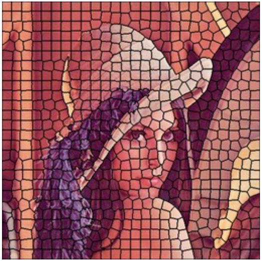

Decomposition 1

Decomposition 2

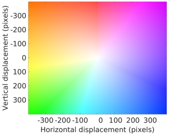

Optical flow representation

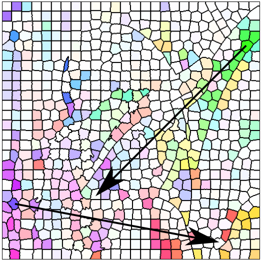

Superpixels

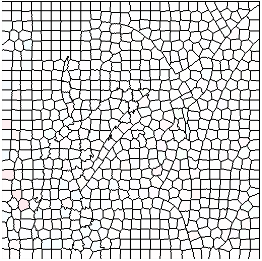

Superpatches

Displacements between the superpixel-based and superpatch-based matches

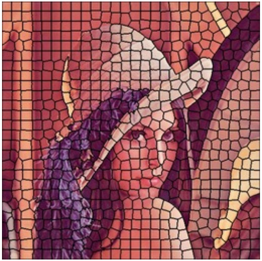

Decomposition 1

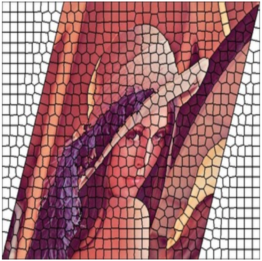

Decomposition 2

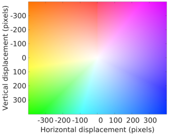

Optical flow representation

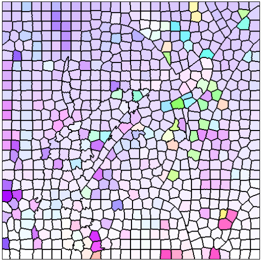

Superpixels

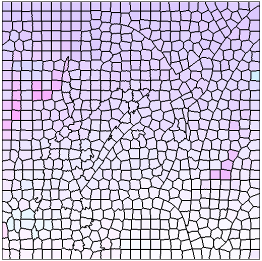

Superpatches

Displacements between the superpixel-based and superpatch-based matches

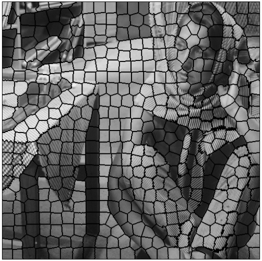

Decomposition 1

Decomposition 2

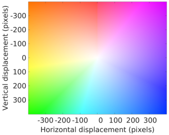

Optical flow representation

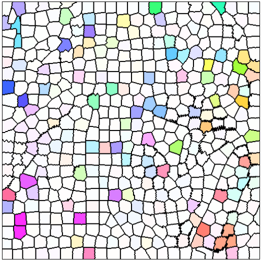

Superpatches (intensity)

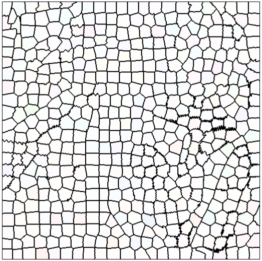

Superpatches (intensity + texture)

Displacements between the superpixel-based and superpatch-based matches

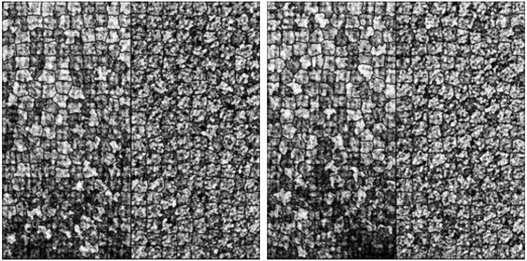

Decomposition 1 Decomposition 2

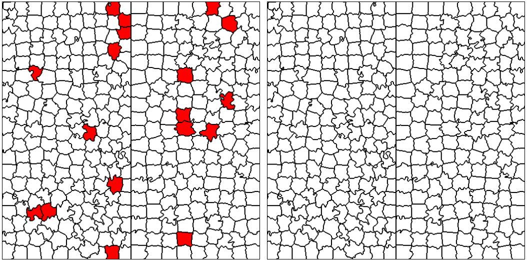

Superpixels Superpatches

Label fusion:

$$L_m(A_i) = \frac{\sum_{T_j \in \mathcal{K}_i^m} \omega(A_i, T_j)}{\sum_{m=1}^{M} \sum_{T_j \in \mathcal{K}_i^m} \omega(A_i, T_j)}$$

$$\omega(A_i, T_j) = \exp\left(1 - \left(\frac{D(\mathbf{A_i}, \mathbf{T_j})}{h(A_i)^2} + \frac{\|c_i - c_j\|_2}{\beta^2}\right)\right)$$

$$\mathcal{L}(A_i) = \underset{m \in \{1,\ldots,M\}}{\text{argmax}} \; L_m(A_i)$$

Superpixels A_i (test), T_j (library)
$\mathcal{K}_i^m = \{T_j\}$ selected, with label m

Measure D between superpatches $\mathbf{A_i}$ and $\mathbf{T_j}$
c_i barycenter of superpixel A_i
$h(A_i)$ minimal distance among the $D(\mathbf{A_i}, \mathbf{T_j})$

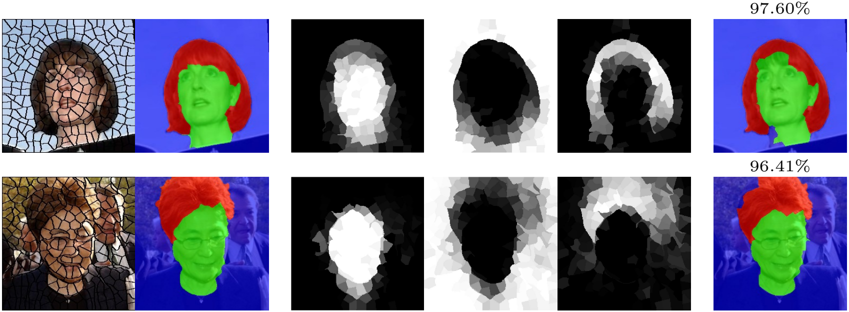

Superpixels | Ground truth | Face | Background | Hair | Result $\mathcal{L}$

Labeling probabilities L_m

SuperPatchMatch - Impact of parameters

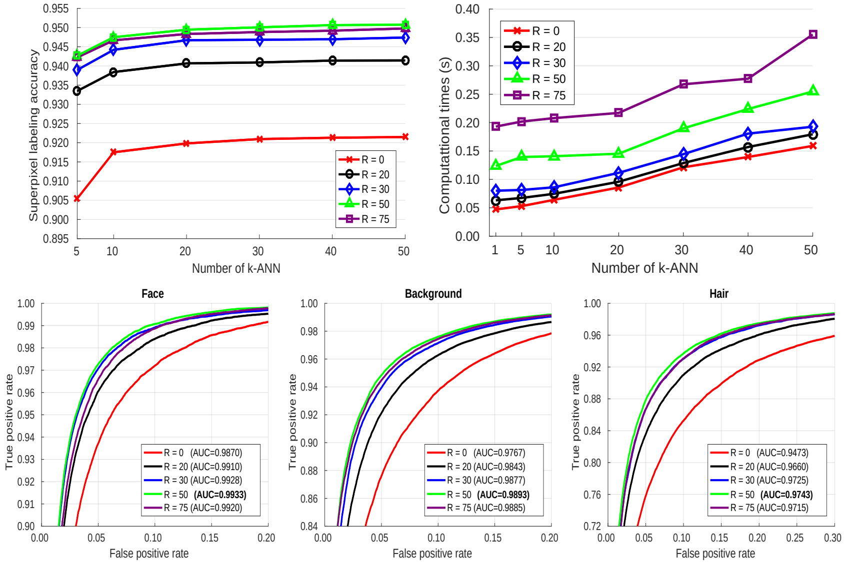

SuperPatchMatch - Impact of parameters

Adaptation of PatchMatch propagation step ($94.20\% \rightarrow 95.08\%$)

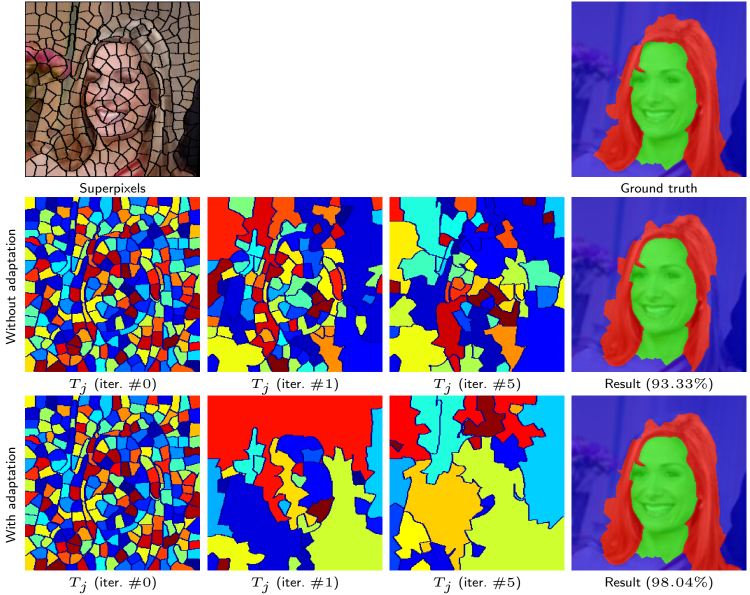

- Comparison to state-of-the-art:

Method	Superpixel-wise accuracy	Pixel-wise accuracy	Computational time
PatchMatch (9×9)	87.73%	87.02%	3.940s
Spatial CRF [Kae et al., 2013]	93.95%	$\times$	$\times$
CRBM [Kae et al., 2013]	94.10%	$\times$	$\times$
GLOC [Kae et al., 2013]	94.95%	$\times$	0.323s
DCNN [Liu et al., 2015]	$\times$	95.24%	$\times$
SuperPatchMatch (2016)	$\mathbf{95.08\%}$	$\mathbf{95.43\%}$	0.255s

$\rightarrow$ Similar results to learning-based approaches

- Impact of regularity:

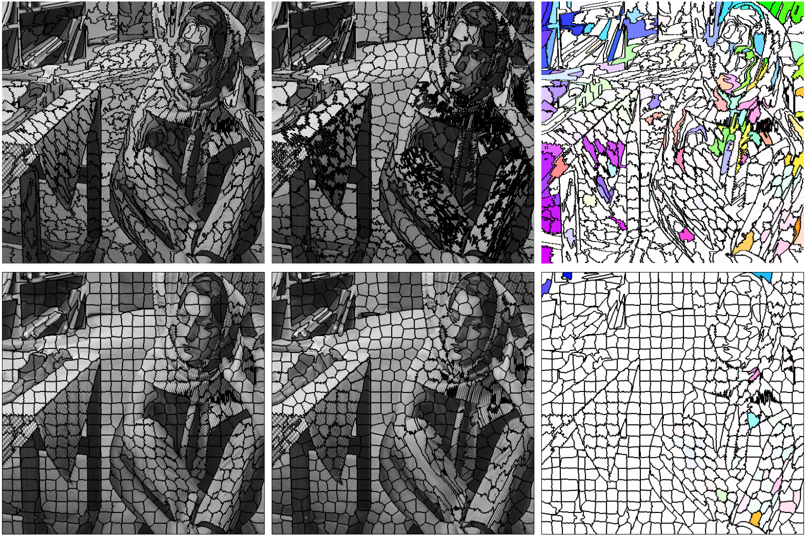

Annex

Decomposition into regular superpixels

Advantages of superpixels:

- Reduce the number of considered elements
- Robustness to noise
- Respect of image objects contours

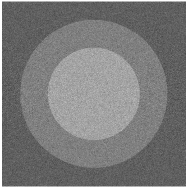

Image

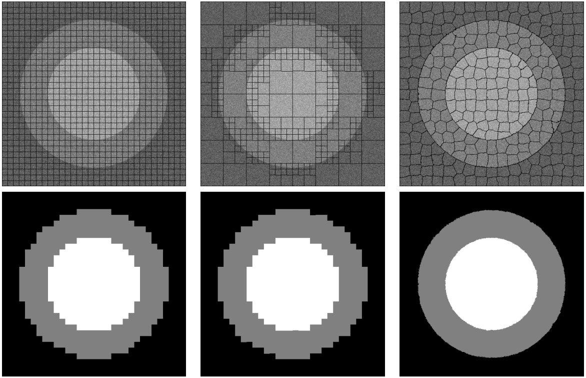

Regular blocks (N=1024)

Quadtree (N=400)

Superpixels (N=289)

Use of superpixels

Advantages of superpixels:

- Reduce the number of considered elements
- Robustness to noise
- Respect of image objects contours

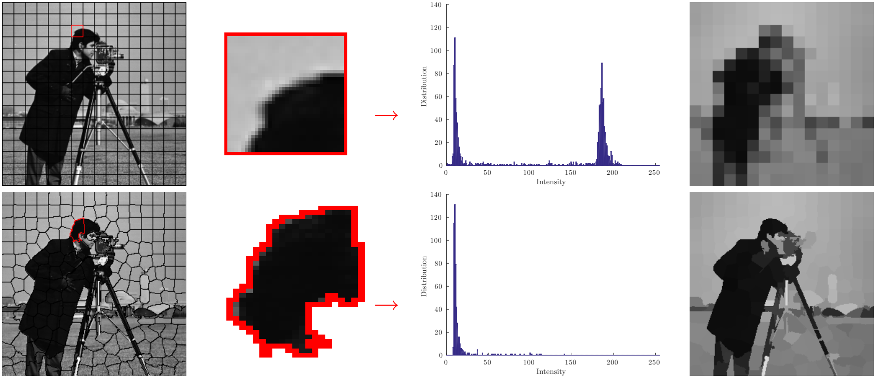

Decomposition | Element | Intensity histogram | Average colors

Advantages of superpixels:

- Reduce the number of considered elements
- Robustness to noise
- Respect of image objects contours

Limitations:

- Shape irregularity → Irregularity of the neighborhood

  → Need for regular superpixels

Decomposition into superpixels

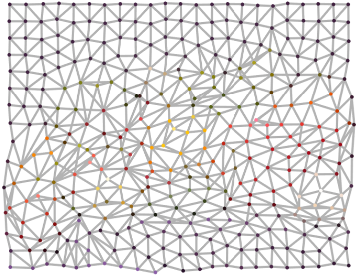

Adjacency graph

Color distance on the neighborhood:

$$d_{\text{neigh.}}(V(p), S_k) = \sum_{q \in V(p)} d_{\text{color}}(F_q, F_{S_k}) w_{p,q}$$

$$w_{p,q} = \frac{1}{Z} \exp\left(-\frac{d_{\text{color}}(F_q, F_{S_k})}{\sigma^2}\right)$$

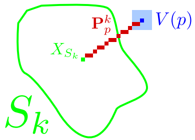

Color distance on linear path:

$$d_{\text{contour}}(\mathbf{P}_p^k) = 1 + \gamma \max_{q \in \mathbf{P}_p^k} \mathcal{C}(q)$$

Total color distance:

$$D_{\text{couleur}}(V(p), S_k, \mathbf{P}_p^k) = \lambda d_{\text{neigh.}}(V(p), S_k) + (1-\lambda) \frac{1}{|\mathbf{P}_p^k|} \sum_{q \in \mathbf{P}_p^k} d_{\text{color}}(q, S_k)$$

Final distance:

$$D(p, S_k) = \left(D_{\text{color}}(V(p), S_k, \mathbf{P}_p^k) + d_{\text{spatial}}(X_p, X_{S_k}) m\right) d_{\text{contour}}(\mathbf{P}_p^k)$$

The distance $d_{\text{neigh.}}$ on the neighborhood $V(p)$ of pixel p can be computed in $\mathcal{O}(1)$.

Demonstration:

The distance between features F in $d_{\text{neigh.}}$ reads:

$$\begin{aligned} d_{\text{neigh.}}(V(p), S_k) &= \sum_{q \in V(p)} (F_q - F_{S_k})^2 w_{p,q}, \\ &= \sum_{q \in V(p)} \left(F_q^2 + F_{S_k}^2 - 2F_q F_{S_k}\right) w_{p,q}, \\ &= \sum_{q \in V(p)} F_q^2 w_{p,q} + \sum_{q \in V(p)} F_{S_k}^2 w_{p,q} - 2 \sum_{q \in V(p)} F_q F_{S_k} w_{p,q}, \\ &= \mathcal{F}_p{}^{(2)} + F_{S_k}^2 \sum_{q \in V(p)} w_{p,q} - 2F_{S_k} \sum_{q \in V(p)} F_q w_{p,q}, \\ &= \mathcal{F}_p{}^{(2)} + F_{S_k}^2 - 2F_{S_k} \mathcal{F}_p{}^{(1)}. \end{aligned}$$

$\mathcal{F}_p{}^{(2)} = \sum_{q \in V(p)} F_q^2$, and $\mathcal{F}_p{}^{(1)} = \sum_{q \in V(p)} F_q$, can be pre-computed.
The complexity of $d_{\text{neigh.}}$ is hence reduced to $\mathcal{O}(1)$ instead of $\mathcal{O}(N)$.

Path between a pixel p at position X_p and a superpixel S_k of barycenter X_{S_k}

Real-time computation with the [Bresenham, 1965] algorithm

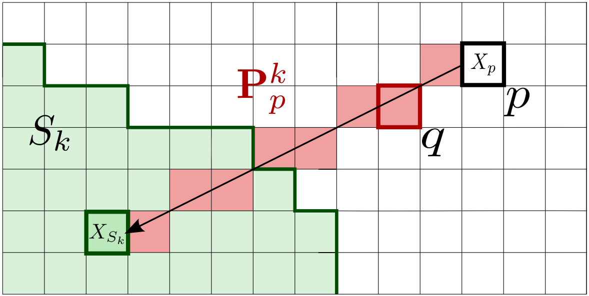

The SCALP method - Comparison to geodesic distances

Sinuous path with geodesics → more irregular superpixels

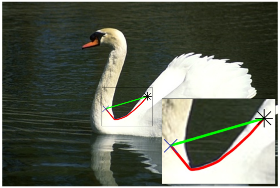

Image

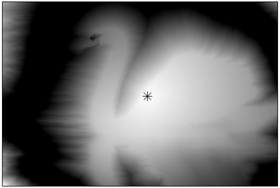

Geodesic distance

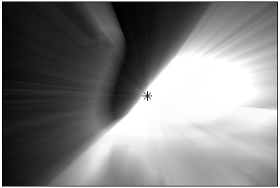

Linear path distance

Image

[Rubio et al., 2016]
(geodesic)

SCALP
(linear path)

The SCALP method - Algorithm

SCALP$(I, K, \mathcal{C})$

Initialization of features $S_k \leftarrow [F_{S_k}, X_{S_k}]$ from a regular grid
Initialization of superpixel labels $\mathcal{S} \leftarrow 0$
Pre-computation of features ${\mathcal{F}_p}^{(2)}$ and ${\mathcal{F}_p}^{(1)}$
For *each iteration* **do**
    Distance $d \leftarrow \infty$
    For *each* S_k **do**
        For *each pixel* p *in a* $(2r+1)\times(2r+1)$ *window centered on* X_{S_k} **do**
            Computation of the linear path $\mathbf{P}_p^k$ [Bresenham, 1965]
            Computation of $D(p, S_k)$ using $\mathcal{C}$ and $\mathbf{P}_p^k$
            If $D(p, S_k) < d(p)$ **then**
                $d(p) \leftarrow D(p, S_k)$
                $\mathcal{S}(p) \leftarrow k$
    For *each* S_k **do**
        Update $[F_{S_k}, X_{S_k}]$
Return $\mathcal{S}$

The SCALP method - Influence of parameters

- Distance parameters

  Neighborhood $|V(p)| = (2n+1)^2$, λ color distance, γ contour distance

Initial image

$n{=}0$, $\lambda{=}1$, $\gamma{=}0$

$n{=}3$, $\lambda{=}1$, $\gamma{=}0$

neighborhood

$n{=}3$, $\lambda{=}0.5$, $\gamma{=}0$

color distance

$n{=}3$, $\lambda{=}0.5$, $\gamma{=}50$

contour distance

The SCALP method - Influence of parameters

- Distance parameters

  Neighborhood $|V(p)| = (2n+1)^2$, λ color distance, γ contour distance

Initial images

Noisy images

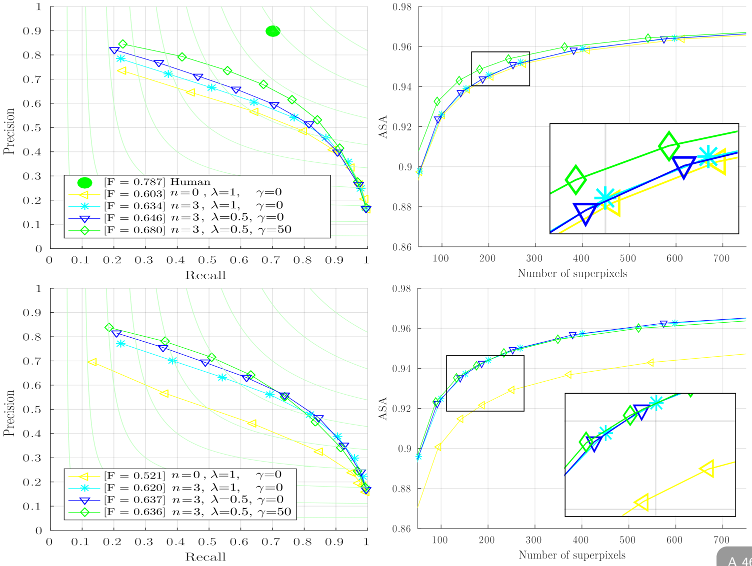

- Contour detection

  Even a simple contour detection from the superpixel boundaries obtained at multiple scales improves the performances.

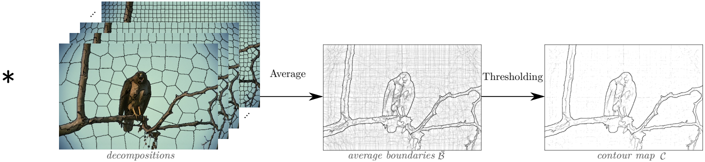

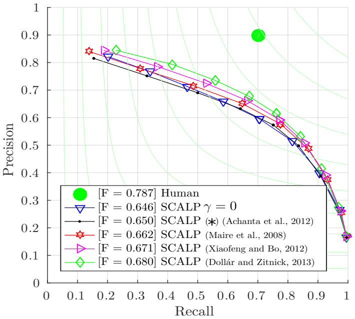

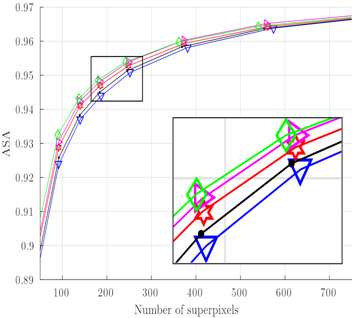

Hard constraint on the initial segmentation

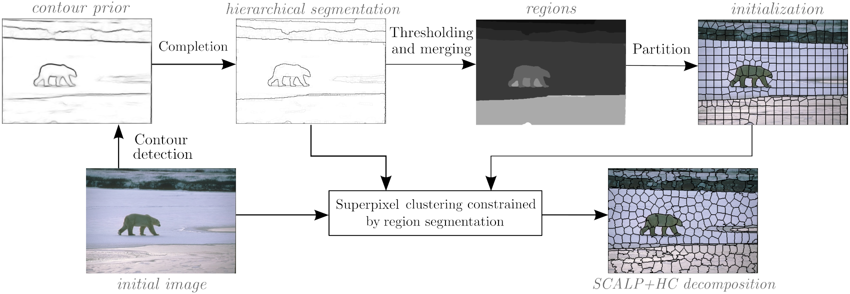

Hierarchical segmentation from a contour map [Arbelaez et al., 2009]
Thresholding of the segmentation by a parameter τ

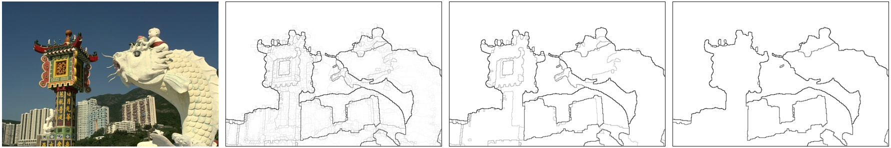

Image $\quad\tau = 0\quad \tau = 0.2 \quad \tau = 0.6$

The SCALP method - Initial segmentation constraint

Adaptation of the hierarchical segmentation to the superpixel scale

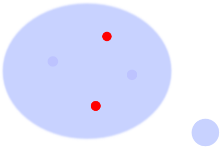

Image

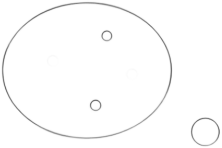

Contour map

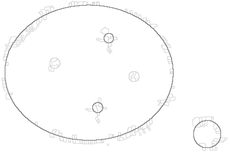

Hierarchical segmentation

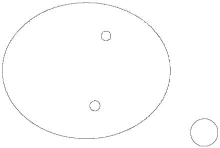

Thresholding

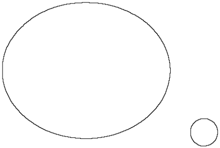

Fusion

Initial images of the BSD

SCALP

SCALP+HC

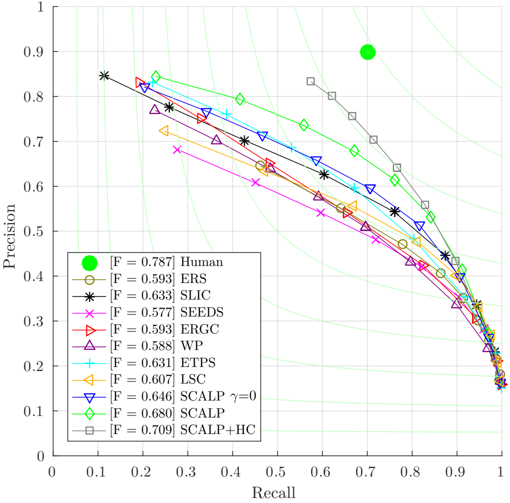

SEEDS [Van den Bergh et al., 2012] and WP [Machairas et al., 2015] added to the comparison

Initial images of the BSD + Gaussian noise

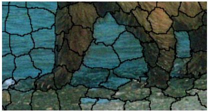

SCALP

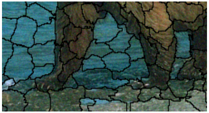

SCALP+HC

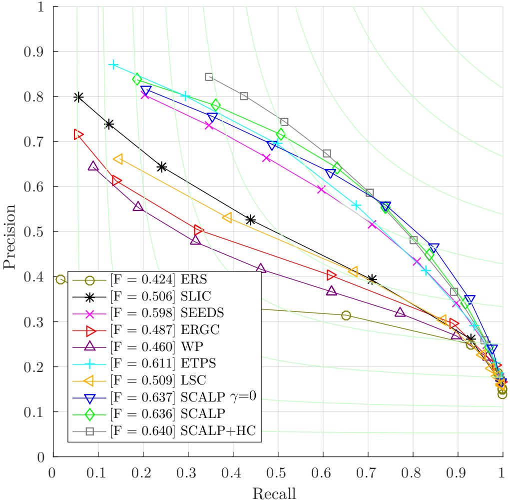

SEEDS [Van den Bergh et al., 2012] and WP [Machairas et al., 2015] added to the comparison

The SCALP method - Results

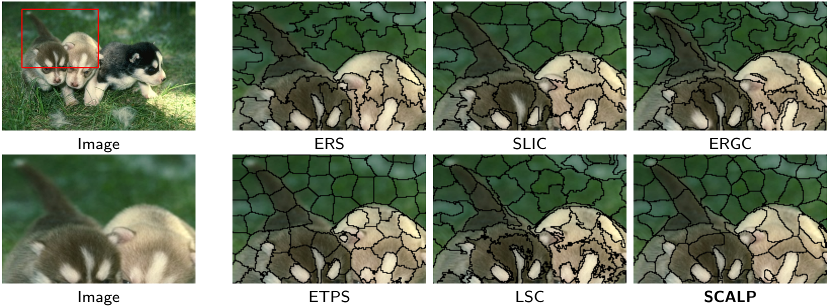

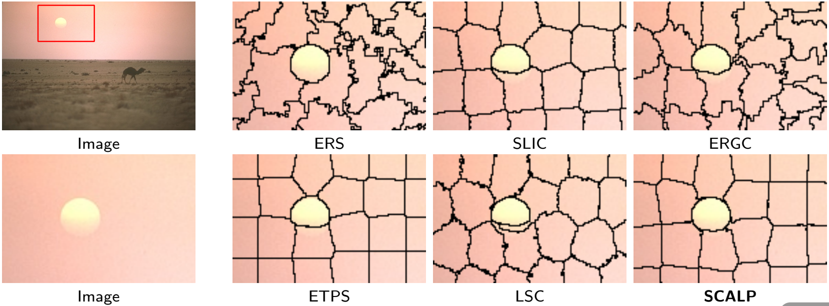

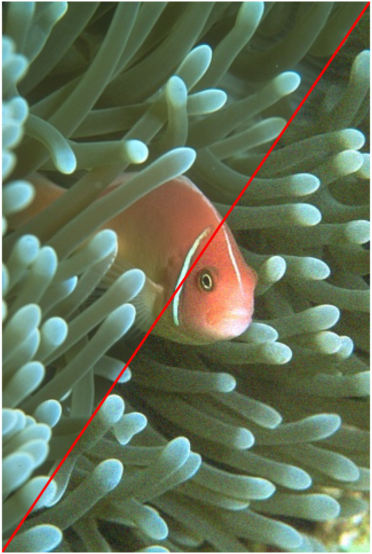

Image / Noisy image

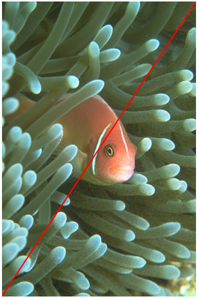

Image / Noisy image

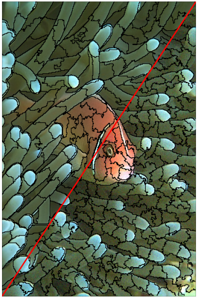

ERS

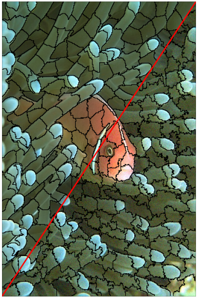

SLIC

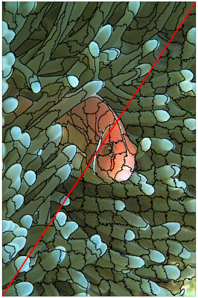

ERGC

ETPS

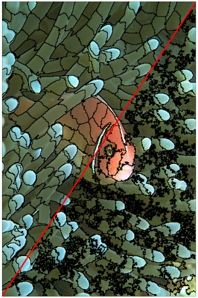

LSC

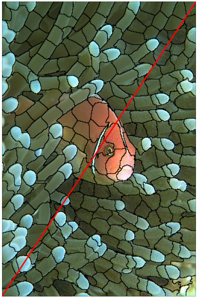

SCALP

The SCALP method - Results on noisy images

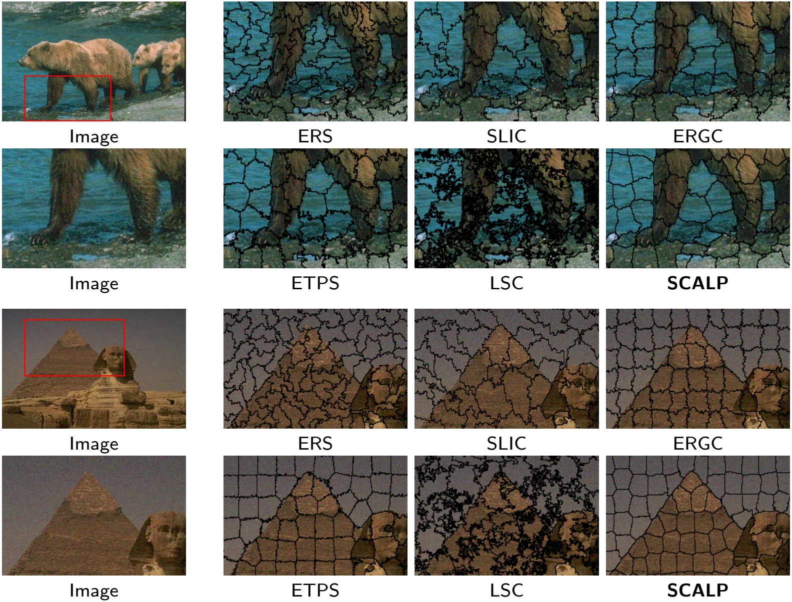

Natural extension to supervoxels for the decomposition of 3D objects

Results on the BRATS dataset [Menze et al., 2015] (MRI with tumors)

ASA 3D:

- SLIC 0.9840 [Achanta et al., 2012]
- ERCG 0.9652 [Buyssens et al., 2014]
- SCALP 0.9848

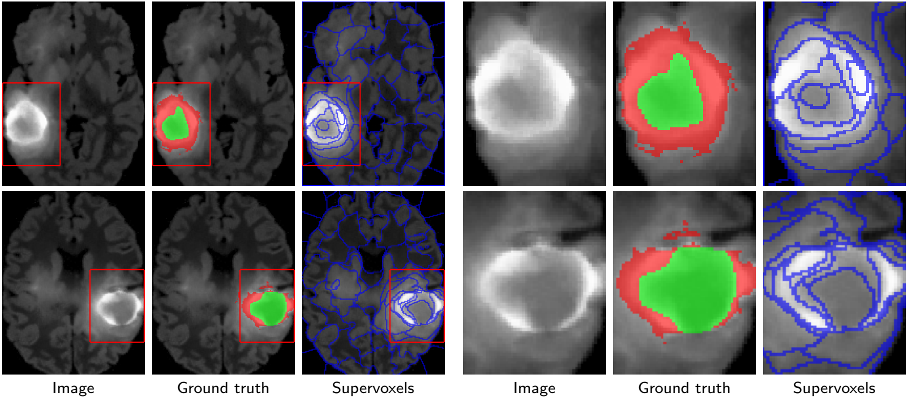

The metrics cannot be simultaneously optimized.

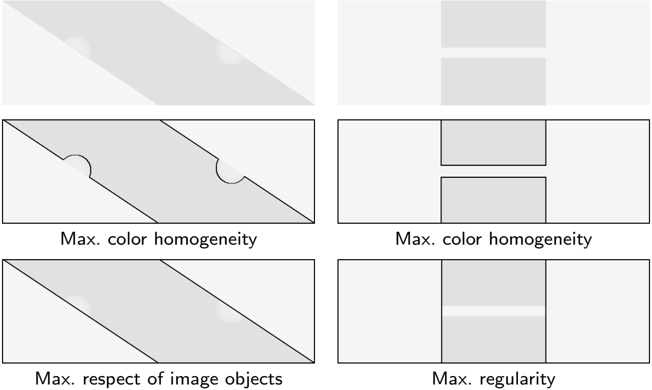

Superpixel metrics

Segmentation into superpixels $\mathcal{S}$, ground truth segmentation $\mathcal{G}$

Global Regularity (GR): Shape regularity and consistency of superpixels

$$\mathsf{SRC}(\mathcal{S}) = \sum_k \frac{|S_k|}{|I|} \cdot \frac{|S|}{|H_S|} \cdot \frac{|\mathsf{P}(H_S)|}{|\mathsf{P}(S)|} \cdot \frac{\min(\sigma_x, \sigma_y)}{\max(\sigma_x, \sigma_y)}$$

$$\mathsf{SMF}(\mathcal{S}) = 1 - \sum_{S_k} \frac{|S_k|}{|I|} \cdot \left\| \frac{S^*}{|S^*|} - \frac{S_k^*}{|S_k^*|} \right\|_1 /2$$

$$\mathsf{GR}(\mathcal{S}) = \mathsf{SRC}(\mathcal{S})\mathsf{SMF}(\mathcal{S})$$

Precision-Recall (PR): Average of superpixels boundaries at multiple scales [Martin et al., 2004]

$$\mathsf{BR}(\mathcal{S},\mathcal{G}) = \frac{|\mathcal{B}(\mathcal{S}) \cap \mathcal{B}(\mathcal{G})|}{|\mathcal{B}(\mathcal{G})|} \qquad \mathsf{P}(\mathcal{S},\mathcal{G}) = \frac{|\mathcal{B}(\mathcal{S}) \cap \mathcal{B}(\mathcal{G})|}{|\mathcal{B}(\mathcal{S})|} \qquad \mathsf{F} = \frac{2.\mathsf{P}.\mathsf{BR}}{\mathsf{P} + \mathsf{BR}}$$

Achievable Segmentation Accuracy (ASA): Respect of the image objects [Liu et al., 2011]

$$\mathsf{ASA}(\mathcal{S},\mathcal{G}) = \frac{1}{|I|} \sum_k \max_i |S_k \cap G_i|$$

Contour Density vs Boundary Recall (CD vs BR): Adherence to contours [Martin et al., 2004]

$$\mathsf{CD}(\mathcal{S}) = \frac{|\mathcal{B}(\mathcal{S})|}{|I|} \qquad \mathsf{BR}(\mathcal{S},\mathcal{G}) = \frac{|\mathcal{B}(\mathcal{S}) \cap \mathcal{B}(\mathcal{G})|}{|\mathcal{B}(\mathcal{G})|}$$

Superpixels metrics - CD vs BR

Contour Density vs Boundary Recall (CD vs BR): [Martin et al., 2004]

$$\mathrm{CD}(\mathcal{S}) = \frac{|\mathcal{B}(\mathcal{S})|}{|I|} \qquad \mathrm{BR}(\mathcal{S},\mathcal{G}) = \frac{|\mathcal{B}(\mathcal{S}) \cap \mathcal{B}(\mathcal{G})|}{|\mathcal{B}(\mathcal{G})|}$$

Image with the ground truth contours

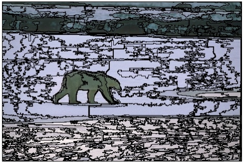

Irregular superpixels (BR=1.00 | BR×(1-CD)=0.563)

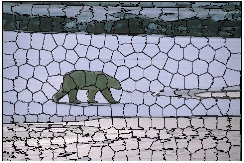

Regular superpixels (BR=1.00 | BR×(1-CD)=0.858)

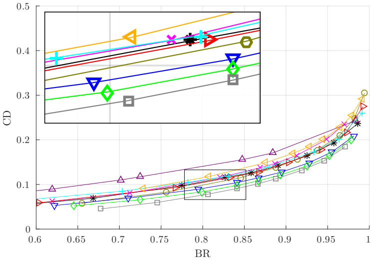

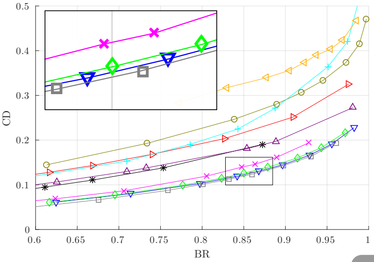

Superpixel metrics - Color homogeneity

Segmentation into superpixels $\mathcal{S}$

Intra-Cluster Variation (ICV): [Benesova and Kottman, 2014]

$$\text{ICV}(\mathcal{S}) = \frac{1}{|\mathcal{S}|}\sum_{S_k}\frac{1}{|S_k|}\sqrt{\sum_{p\in S_k}(I(p)-\mu(S_k))^2}$$

Explained Variation (EV): [Moore et al., 2008]

$$\text{EV}(\mathcal{S}) = \frac{\sum_{S_k}|S_k|\left(\mu(S_k)-\mu(I)\right)^2}{\sum_{p\in I}\left(I(p)-\mu(I)\right)^2} = 1-\sum_{S_k}\frac{|S_k|}{|I|}.\frac{\sigma(S_k)^2}{\sigma(I)^2}$$

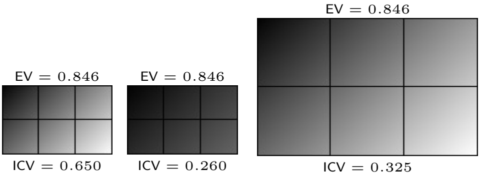

Segmentation into superpixels $\mathcal{S}$

Intra-Cluster Variation (ICV): [Benesova and Kottman, 2014]

$$\text{ICV}(\mathcal{S}) = \frac{1}{|\mathcal{S}|}\sum_{S_k}\frac{1}{|S_k|}\sqrt{\sum_{p\in S_k}(I(p)-\mu(S_k))^2}$$

Explained Variation (EV): [Moore et al., 2008]

$$\text{EV}(\mathcal{S}) = \frac{\sum_{S_k}|S_k|\,(\mu(S_k)-\mu(I))^2}{\sum_{p\in I}(I(p)-\mu(I))^2} = 1-\sum_{S_k}\frac{|S_k|}{|I|}.\frac{\sigma(S_k)^2}{\sigma(I)^2}$$

Superpixels

Average colors $\mu(S_k)$

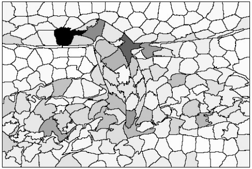

Color variance $\sigma(S_k)^2$

Segmentation into superpixels $\mathcal{S}$

Intra-Cluster Variation (ICV): [Benesova and Kottman, 2014]

$$\mathrm{ICV}(\mathcal{S}) = \frac{1}{|\mathcal{S}|} \sum_{S_k} \frac{1}{|S_k|} \sqrt{\sum_{p \in S_k} (I(p) - \mu(S_k))^2}$$

Explained Variation (EV): [Moore et al., 2008]

$$\mathrm{EV}(\mathcal{S}) = \frac{\sum_{S_k} |S_k| \, (\mu(S_k) - \mu(I))^2}{\sum_{p \in I} (I(p) - \mu(I))^2} = 1 - \sum_{S_k} \frac{|S_k|}{|I|} . \frac{\sigma(S_k)^2}{\sigma(I)^2}$$

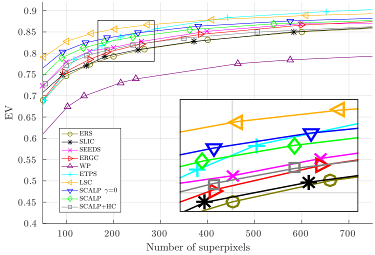

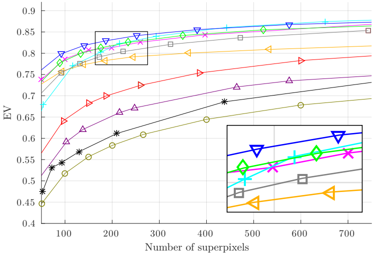

- Shape regularity

Circularity (C) [Schick et al., 2012]:

$$\mathrm{C}(S) = \frac{4\pi|S|}{|P(S)|^2}$$

Shape Regularity Criteria (SRC):

$$\mathrm{SRC}(S) = \frac{|S|}{|H_S|}\cdot\frac{|\mathrm{P}(H_S)|}{|\mathrm{P}(S)|}\cdot\frac{\min(\sigma_x,\sigma_y)}{\max(\sigma_x,\sigma_y)}$$

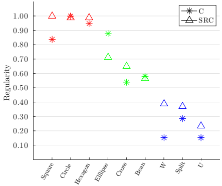

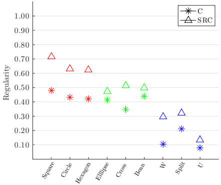

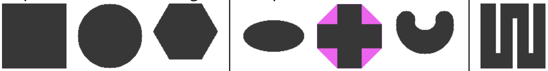

	Regular shapes			Standard shapes			Irregular shapes		
	Square	*Circle*	*Hexagon*	*Ellipse*	*Cross*	*Bean*	*W*	*Split*	*U*
C	0.830	1.000	0.940	0.870	0.530	0.580	0.150	0.280	0.150
SRC	**1.000**	**0.989**	**0.987**	**0.712**	**0.650**	**0.564**	**0.387**	**0.369**	**0.233**

	Square	Circle	Hexagon	Ellipse	Cross	Bean	W	Split	U
C	0.480	0.430	0.420	0.410	0.340	0.440	0.100	0.210	0.070
SRC	**0.716**	**0.633**	**0.625**	**0.474**	**0.515**	**0.500**	**0.296**	**0.321**	**0.136**

- Robustness to noise

  SLIC superpixels with noise on the boundaries

C = 0.296 | SRC = 0.434

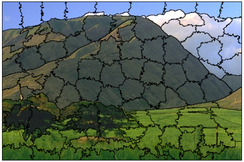

$m = 10$

C = 0.401 | SRC = 0.562

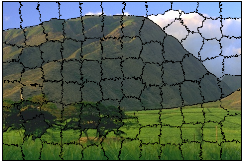

$m = 50$

C = 0.371 | SRC = 0.570

$m = 200$

- Robustness to noise

SLIC superpixels with noise on the boundaries

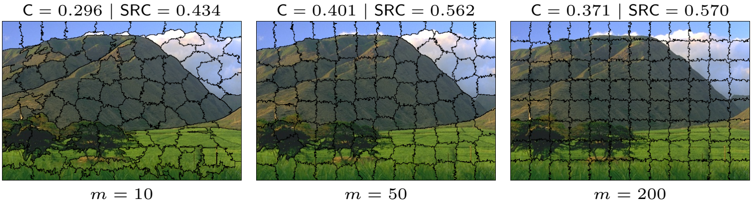

Evolution of the regularity parameter m
Average results on the BSD

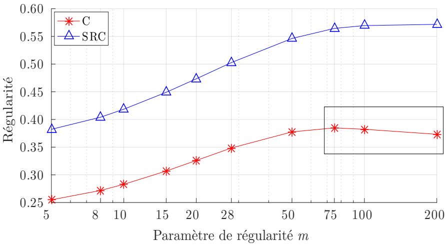

- Evaluation of the superpixel decomposition consistency

Jaccard [Machairas et al., 2015]:

$$\mathsf{J}(\mathcal{S}) = \frac{1}{|\mathcal{S}|} \sum_{S_k \in \mathcal{S}} \frac{|S_k^* \cap \hat{S}^*|}{|S_k^* \cup \hat{S}^*|}$$

$$\hat{S}^* = S^*_{\underset{t}{\mathrm{argmax}}(|S_t^*| \geq \frac{|I|}{|\mathcal{S}|})}$$

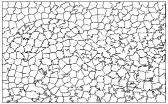

Decomposition $\mathcal{S}$

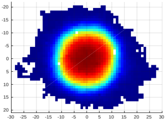

Average shape S^*

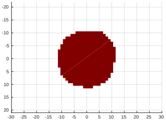

Binary average shape $\hat{S}^*$

→ Does not consider the size of superpixels. Thresholding not robust to large superpixels.

Smooth Matching Factor (SMF):

$$\mathsf{SMF}(\mathcal{S}) = 1 - \sum_{S_k} \frac{|S_k|}{|I|} \cdot \left\| \frac{S_k^*}{|S_k^*|} - \frac{S^*}{|S^*|} \right\|_1 /2$$

→ Direct comparison to the average shape S^*

→ More relevant and robust metric

$\mathsf{J} = 0.331$

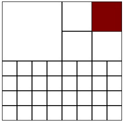

$\mathsf{SMF} = 0.520$

$\mathsf{J} = 0.308$

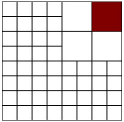

$\mathsf{SMF} = 0.719$

$\mathsf{J} = 0.262$

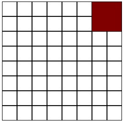

$\mathsf{SMF} = 0.912$

$\mathsf{J} = 0.364$

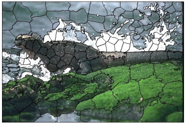

$\mathsf{SMF} = 0.517$

$\mathsf{J} = 0.291$

$\mathsf{SMF} = 0.536$

- Global evaluation of the regularity: shape and consistency

Global Regularity (GR):

$$\text{GR}(\mathcal{S}) = \text{SMF}(\mathcal{S}) \sum_{S_k \in \mathcal{S}} \frac{|S_k|}{|I|} \text{SRC}(S_k)$$

→ SCALP generates very regular superpixels while respecting the image contours.

→ The evaluation of performances at several regularity levels enables to be robust to the choice of the regularity parameter and to better represent a superpixel method potential.

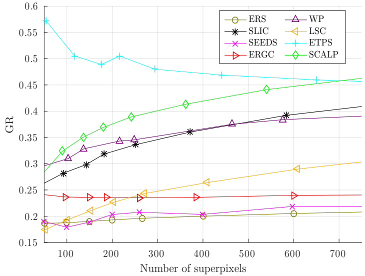

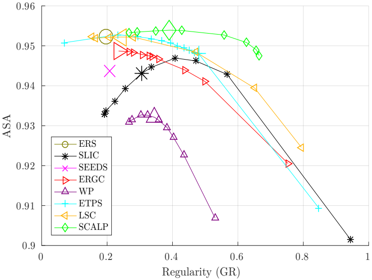

The regularity of superpixels facilitates the tracking of objects.

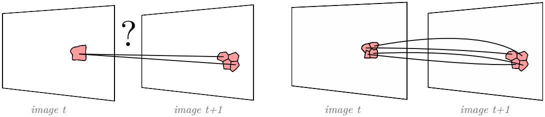

Tracking accuracy with the TSP method [Chang et al., 2013] on the sequences from [Tsai et al., 2012].

	Accuracy		Loss	
Sequence	Regular	Irregular	Regular	Irregular
birdfall2	98.3%	97.8%	1.0%	1.4%
girl	51.1%	50.4%	13.9%	24.8%
parachute	75.3%	73.9%	4.5%	5.1%
penguin	94.3%	85.0%	2.6%	8.8%
Average	79.8%	76.7%	5.5%	10.0%

The regularity of superpixels facilitates the tracking of objects.

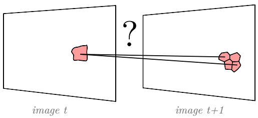

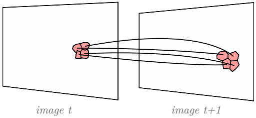

Tracking accuracy with the TSP method [Chang et al., 2013] on the sequences from [Tsai et al., 2012].

	Accuracy		Loss	
Sequence	Regular	Irregular	Regular	Irregular
birdfall2	98.3%	97.8%	1.0%	1.4%
girl	51.1%	50.4%	13.9%	24.8%
parachute	75.3%	73.9%	4.5%	5.1%
penguin	94.3%	85.0%	2.6%	8.8%
Average	79.8%	76.7%	5.5%	10.0%

The irregularity facilitate the approximation of the initial colors.
Colors contained into a superpixel approached by a third order polynomial.


Initial image I

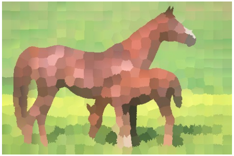
Regular compression I_r


Irregular compression I_r

Average on the BSD images [Martin et al., 2001]

Mean Square Error (MSE):

$$\text{MSE}(I, I_r) = \frac{1}{|I|} \sum_{p \in I} (I(p) - I_r(p))^2$$

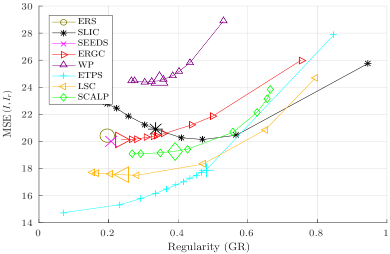

The regularity is correlated to performances.

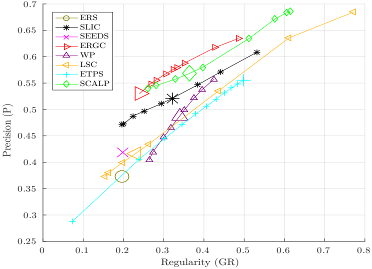

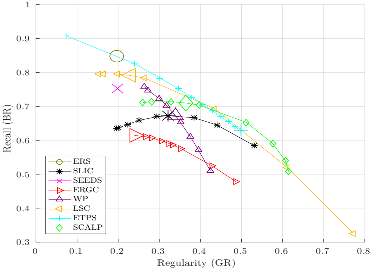

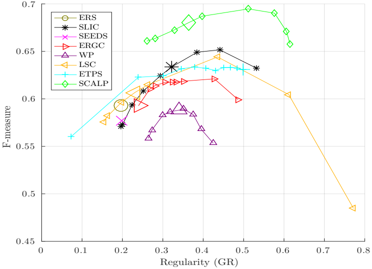

Impact of regularity - Image segmentation

The fusion of irregular decompositions may enable to efficiently segment the image objects.

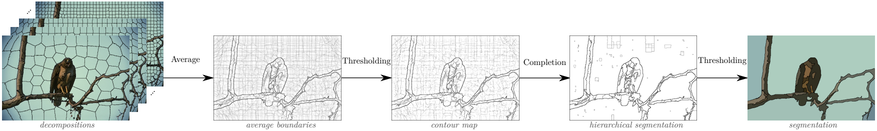

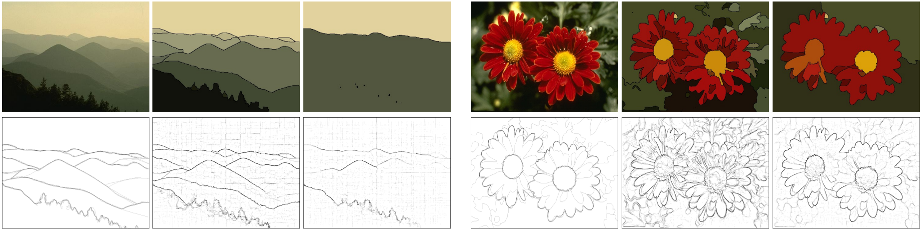

Images / contours | Low regularity | High regularity | Images / contours | Low regularity | High regularity

Impact of regularity - Correlation

Higher correlation between the proposed metrics and the performances.

	GR	SMF	J	SRC	C
ASA	$-\mathbf{0.5473}$	-0.5250	-0.5266	-0.5350	-0.5318
UE	$\mathbf{0.5506}$	0.5284	0.5299	0.5384	0.5353
BR	$-\mathbf{0.9136}$	-0.8974	-0.8972	-0.9049	-0.9034
P	-0.9627	-0.9645	-0.9656	-0.9688	$-\mathbf{0.9712}$
EV	$-\mathbf{0.6641}$	-0.6426	-0.6428	-0.6528	-0.6503
MSE	$\mathbf{0.6760}$	0.6552	0.6554	0.6655	0.6636
Average	$\mathbf{0.8165}$	0.8113	0.8076	0.8122	0.8085

Annex

Perspectives

Perspectives - Synthesis of non-linear transformation

→ To adapt OPAL to the transfer of displacement vectors

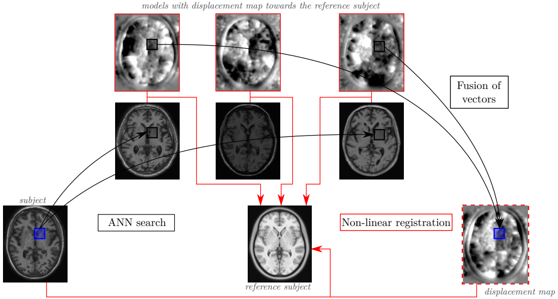

Smart fusion of displacement vectors:

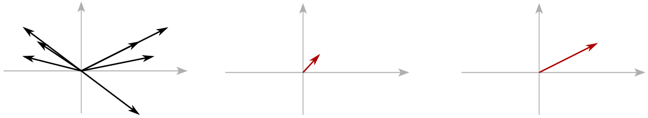

Set of vectors | Average vector | Median vector [Liu, 2013]

Previous works: Smart fusion of optical flow vectors [Fortun et al., 2016]
Patch-based synthesis of non-linear transformations [Kim et al., 2015]

- Supervoxel-based segmentation of 3D medical images
  - → To adapt SuperPatchMatch for complex structures, *e.g.*, tumors:
    - — No prior on tumor position
    - — Contours correlated to the MRI image content

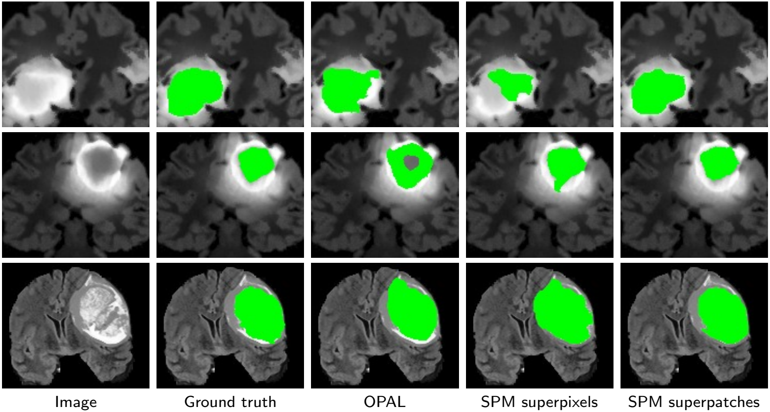

Example of 2D segmentation of tumors on the BRATS dataset [Menze et al., 2015]

Patch-based method [Frigo et al., 2016]:

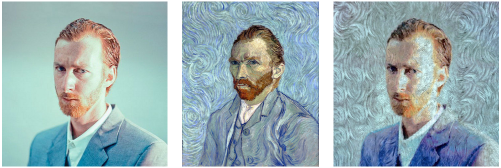

Target image Source image Result

→ Important computational time
→ Copy of the same image parts
→ Transfer of texture and colors = too strict respect of the target contours

→ Superpixels to reduce the computational cost
→ Constrained search for matches (SCT)
→ To force the capture of the image contours

Distance *inversed* SCALP:

$$D(p, S_k) = \left(d_{\text{spatial}}(p, S_k)m - D_c(V(p), S_k, \mathbf{P}_p^k)\right) \frac{1}{d_{\text{contour}}(\mathbf{P}_p^k)}$$

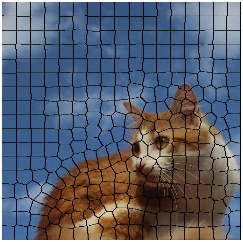

inversed SCALP

Comparison to neural network:

Target image

Source image

Patch-based method
[Frigo et al., 2016]

Neural network
[Gatys et al., 2015]